

POLITECNICO DI TORINO

Master's Degree in Biomedical Engineering



**Politecnico
di Torino**

Master's Degree Thesis

**Enhancement of Readiness Potentials'
Pre-Processing Chain in a
Brain-Computer Interface for
nonresponsive patients**

Supervisors

Prof. Gabriella OLMO

Prof. Vito DE FEO

Candidate

Chiara BOTRUGNO

July 2022

Abstract

Over the last years, an increasing number of patients survive severe brain injury thanks to recent improvements in intensive care. Nevertheless, the recovery of brain capacities and motor skills is not always complete: it may happen that the patient maintains vital functions but does not show overt awareness of himself and the environment around them. From the diagnostic point of view, behavioral assessments can provide general and summary information on the patient's state of consciousness, based on evidence found in attitudes and responses, voluntary or not. Despite this, such type of assessment can lead to a relevant number of misdiagnoses or inaccurate diagnoses, depending on the severity of brain injury, which may reveal incomplete or inconsistent behaviors.

The challenge is to design a low-cost non-invasive assessment method that, starting from electroencephalographic (EEG) and electromyographic (EMG) signals, can detect and distinguish different levels of consciousness. This method relies on a detailed pre-processing chain, which allows to clean up raw signals and bring to light the real information contained in the biopotential. This information is then fed to the machine learning algorithms that allow classification, useful for differential diagnosis.

The following thesis focuses on some steps of the pre-processing chain, in order to improve the quality of the obtained Readiness Potential (RP), allowing a more accurate classification.

In particular, the covered topics are: (1) set-up of temporal filtering parameters, in order to extract from raw EEG signal the frequency bands which contain useful information; (2) implementation of a novel method for jitter compensation based on Residue Iteration Decomposition (RIDE), an algorithm of iterative subtraction which separates different clusters of ERP's components according to their time-locking to stimulus onset, response times, or estimated latencies and reconstructs ERPs by re-aligning the component clusters to their most probable trial latencies; (3) comparison of RIDE method with the previous Woody's method and testing alternative methods which combine both techniques for jitter compensation, relying on the strengths and weaknesses of each of them; (4) analysis of event-related potentials from patients with hemiplegia in order to assess the robustness of the pre-processing chain.

Table of Contents

List of Tables	IV
List of Figures	V
1 Consciousness: definition, physiology and pathologies	1
1.1 Consciousness: a mystery to be solved	1
1.2 Neural correlates of consciousness	2
1.3 Levels of consciousness	3
1.3.1 Disorders of consciousness	5
1.3.2 Behavioral assessment methods	6
1.3.3 Instrumental assessment methods	8
2 Consciousness measurement: EEG signal and Movement-Related Cortical Potentials (MRCP)	15
2.1 Biosignals: Electroencephalography and Electromyography	16
2.1.1 EEG signals	16
2.1.2 EMG signals	19
2.2 Conscious intention and motor cognition	23
2.2.1 Readiness Potential (RP) or Bereitschaftspotential	26
2.2.2 Lateralized Readiness Potential (LRP)	29
2.2.3 Libet's Experiment	31
3 Readiness Potential Recording: Materials and Methods	33
3.1 Tasks and Protocols	34
3.1.1 2012-2015 Protocol	34
3.1.2 2015-2018 Protocol	35
3.1.3 2018 Protocol	35
3.1.4 Datasets: classification	36
3.2 Experimental setup	37
3.3 Software for signal processing	39
3.3.1 EEGLAB	39

3.3.2	MRCPLAB	40
4	Jitter Compensation	44
4.1	Trial-to-trial latency variability	44
4.2	Previous attempts	46
4.2.1	Woody’s Method	48
4.3	Residue Iteration Decomposition (RIDE)	50
4.3.1	ERP model	51
4.3.2	Algorithms and Methods	52
4.3.3	Input Parameters and Output Variables	57
4.3.4	Results and Plots	59
4.3.5	Comparing Methods: Woody’s Method vs. RIDE Method	65
4.3.6	Combining Methods: Woody’s and RIDE in cascade	71
4.4	Discussion	76
4.4.1	Limitations and Future Challenges	77
5	ERP Temporal Filtering	79
5.1	Methods and Results	79
5.2	Discussion	83
6	Conclusions and Ideas for the Future	86
6.1	Case study on a patient with Hemiplegia	87
	Bibliography	90

List of Tables

4.1	Different combinations of averaged RPs representing different areas of the brain.	65
4.2	Brain zoning applied to Woody's Method as a reference for epoch realignment.	74

List of Figures

1.1	A two-dimensional representation of consciousness. The X axis represents the Content of Consciousness, the experience of which can vary in vividness. The Y axis represents the Level of Consciousness, or wakefulness, or vigilance, or arousal. Clinical conditions are in red, while normal physiological states are in yellow.	4
1.2	Global brain metabolism detected by FDG-PET in a healthy control (left) and in a patient in an unresponsive wakefulness syndrome (right). Red colorscale indicates regions with high consumption of glucose; blue colorscale indicates regions with low consumption of glucose.[6]	9
1.3	Supplementary motor area activity during tennis imagery in a patient diagnosed as being in a vegetative state and in a healthy volunteer (left). Parahippocampal gyrus, posterior parietal lobe, and lateral premotor cortex activity while imagining moving around a house in the patient and in a healthy volunteer (right).[14]	11
1.4	Neural tracks obtained with DTI in a healthy control (top) and a patient in MCS (bottom) confirms the structural damage which is evident in the temporo-parietal regions of the right hemisphere (bottom right - T1 MRI structural image). Colors indicate directionality of water diffusion: red = left-right; green = anterior-posterior; blue = superior-inferior.[6]	12
2.1	EEG cap for brain potentials recordings.	17
2.2	International Standard 10-20 for electrodes setup in EEG recordings.	18
2.3	Motor Unit (MU) and its innervation.	20
2.4	Motor Unit Action Potential (MUAP) resulting from the summation of fibers' action potentials: with the same motor task, it changes width and shape in dependence on positioning of the electrode compared to the fiber of MU.	21
2.5	Surface EMG electrodes.	22
2.6	Intramuscular EMG recordings.	22

2.7	Cortical areas involved in voluntary motor control.	24
2.8	Computational model for movement execution. Red blocks provide movement selection and prediction, conscious intention and awareness of the action.	25
2.9	Bereitschaftspotential (BP) with the superposition of the Pre-Motor Positivity (PMP) and the Motor Potential (MP):	27
2.10	Representation of the early and late component of a RP.	28
2.11	Topographic distribution of the lateralized current on the scalp when the readiness potential is generated.	29
2.12	Libet's distribution of events that occur at the brain level before a motor task	31
3.1	2018 Protocol for EEG, EOG and EMG recordings (voluntary, semi-voluntary and involuntary task).	36
3.2	Experimental setup in <i>Centro Puzzle</i> , Turin	38
3.3	EEGLAB Graphical User Interface: for this project, the menu MRCPLAB and its sub-menu are used.	40
3.4	MRCPLAB and "Import/Save Data" Menu.	41
3.5	Dataset parametes settings while importing datasets.	42
3.6	MRCPLAB and "EEG Channel Operations" Menu.	43
4.1	Comparing different conditions, the smearing effect of trial-to-trial latency variability induces errors in the resulting averaged waveform.[27] Case 1: Different amplitudes and same latency variability induce indistinguishable difference of amplitude in the final ERP. Case 2: Same amplitudes and different latency variability mimic an erroneous amplitude difference between conditions.	45
4.2	ERPs obtained by averaging single trials with components temporally locked to the stimulus onset (A) or not temporally locked to the stimulus onset (B). [28]	46
4.3	Stimulus-locked and response-locked averaged ERPs – each method smears the other component.	47
4.4	The red dashed signal, corresponding to the most correlated epoch with the first one, was aligned with the signal of the most correlated epoch.	49
4.5	Conventional average ERP (left) from single trials with latency jitter, decomposition by RIDE (middle) and reconstructed ERP after correcting for latency variability (right). [27]	51
4.6	Steps for Decomposition Module using two artificial sinusoidal components for a single electrode. [28]	54
4.7	RIDE algorithm workflow.	56

4.8	Single trial ERP signal referred to C3 channel, in which three components can be identified in the chosen time window.	58
4.9	Illustration of the superposition of S component signals for the whole set of electrodes.	60
4.10	Illustration of the superposition of C component signals for the whole set of electrodes.	61
4.11	Illustration of the superposition of R component signals for the whole set of electrodes.	61
4.12	Separated components for channel C3.	62
4.13	Illustration of the superposition of C component signals for the whole set of electrodes.	63
4.14	Illustration of the superposition of R component signals for the whole set of electrodes.	64
4.15	Separated components for channel C3.	64
4.16	Jitter compensation: Woody's Method	66
4.17	Jitter compensation: RIDE Method	66
4.18	Superposition of methods: Pre-Motor Area	66
4.19	Superposition of methods: Motor Area	66
4.20	Jitter compensation: Woody's Method	67
4.21	Jitter compensation: RIDE Method	67
4.22	Superposition of methods: Pre-Motor Area	67
4.23	Superposition of methods: Motor Area	67
4.24	Jitter Compensation: Woody's Method	68
4.25	Jitter Compensation: RIDE Method	68
4.26	Superposition of methods: Pre-Motor Area	68
4.27	Superposition of methods: Motor Area	68
4.28	Jitter Compensation: Woody's Method	69
4.29	Jitter Compensation: RIDE Method	69
4.30	Superposition of methods: Pre-Motor Area	69
4.31	Superposition of methods: Motor Area	69
4.32	Jitter Compensation: Woody's Method	70
4.33	Jitter Compensation: RIDE Method	70
4.34	Superposition of methods: Pre-Motor Area	70
4.35	Superposition of methods: Motor Area	70
4.36	Woody's Method	71
4.37	RIDE Method	71
4.38	Superposition of methods: Pre-Motor Area	71
4.39	Superposition of methods: Motor Area	71
4.40	Methods in cascade	72
4.41	Superposition of Methods: Motor area	72
4.42	Methods in cascade	72

4.43	Superposition of Methods: Motor area	72
4.44	Methods in cascade	73
4.45	Superposition of Methods: Motor area	73
4.46	Methods in cascade	74
4.47	Superposition of Methods: Motor area	74
4.48	Methods in cascade	75
4.49	Superposition of Methods: Motor area	75
4.50	Methods in cascade	75
4.51	Superposition of Methods: Motor area	75
5.1	RP power spectral density (PSD) computed with spectral resolution of 0.125 Hz.	80
5.2	RP power spectral density (PSD) zooming on frequencies 2-32 Hz.	80
5.3	EEG epoch before any kind of processing, with the superposition of the same epoch filtered at 3 Hz with a FIR filter (order 25).	82
5.4	EEG epoch before any kind of processing, with the superposition of the same epoch filtered at 3 Hz with a IIR filter (order 9).	82
5.5	Jitter compensation applying RIDE method with no temporal filtering.	83
5.6	Jitter compensation applying RIDE method with a 3 Hz low-pass filter inserted before epoch calculation.	83
5.7	Jitter compensation applying RIDE method with 20 Hz low-pass filter before the epoch calculation.	84
5.8	Jitter compensation applying RIDE method with a 20 Hz low-pass filter inserted before epoch calculation and 'smooth' function applied in the end for the visualization.	84
6.1	RP from channels Fc3 and Fc4 while performing Unimanual task.	87
6.2	RP from channels C3 and C4 while performing Unimanual task.	87
6.3	RP from channels Fc3 and Fc4 while performing Bimanual task.	88
6.4	RP from channels C3 and C4 while performing Bimanual task.	88
6.5	Readiness Potential from a hemiplegic subject (Channel C3) with RIDE jitter compensation (blue) and no jitter compensation applied (green).	88

Chapter 1

Consciousness: definition, physiology and pathologies

1.1 Consciousness: a mystery to be solved

Human consciousness, meant as awareness of the person himself and of the environment around, is still a mystery, perhaps one of the greatest in scientific research. Over the decades, scholars have argued that consciousness was impossible to understand scientifically. Today, many authors state that it is “understandable, measurable, replicable and reproducible in artificial intelligences”, which is what this project aspires to.

The term “consciousness” involves different meanings and describes a multiplicity of mental phenomena. It designates vigilance, a state of wakefulness, but also awareness of oneself and of one’s actions. It’s an inner experience that includes sensory perceptions (sounds, colors), body sensations (pleasure, pain), emotions (fear, hate), moods (serenity, sadness).

States of consciousness, which begin upon awakening and end when we fall asleep, occur in the brain predominantly in the thalamic-cortical system. Both consciousness and mind do not have the dimension of space, therefore they escape the laws of scientific investigation of verification and proof. Thoughts, feelings, moods, intentionality are present only in a singular consciousness: they concern subjectivity, which is private, personal, unique.

Many theories have been debated about the origin and significance of human consciousness. “Reductionism” (or physicalism) holds that the activity of consciousness and mind can be studied only if "reduced" to events of the brain: consciousness and mind, therefore, are nothing more than a brain process, a material process, a

physico-chemical event of brain matter, implying an identity between consciousness, mind and brain. “Behaviorism” takes a clear position on the issue, arguing that the best way to deal with it is to avoid any reference to the mind and conscience, as they are not directly observable and quantifiable and are therefore placed outside the scope of scientific investigation: in order to construct a science of behaviour, it is necessary to adopt the methods of physics and biology, which are based on objective and experimental evidence. [1]

All the arguments developed so far show that the subject of consciousness and mind is a difficult problem.

As David Chalmers states, it’s useful to divide the associated problems of consciousness into “hard” and “easy” problems. The easy problems of consciousness are directly susceptible to the standard methods of cognitive science, whereby a phenomenon is explained in terms of computational or neural mechanisms: they concern the explanation of cognitive abilities and functions. The hard problem of consciousness is the problem of experience, in which there is also a subjective aspect: it goes beyond problems about the performance of functions, so that the usual explanatory methods of cognitive science and neuroscience do not suffice. [2] In conclusion, theories so far have not solved the “hard problem” of mind and consciousness, namely how a physical brain can generate a “non-physical essence”.

1.2 Neural correlates of consciousness

From the neurological point of view, talking about consciousness, several aspects can be distinguished:

- a. *Level of vigilance*, that is the general state of attention with which psychic activities are experienced; one can be attentive or distracted while being equally alert, can be asleep while maintaining a certain degree of vigilance and contact with the environment. The structure responsible for fluctuations of vigilance is the reticular formation, placed in the median region of the brain stem.
- b. *Peripheral correlates of consciousness*, that are somatic modifications that accompany the fluctuating of vigilance: they concern palpebral and ocular movements, pupils, spontaneous and reflex body motility, muscle tone and breath. The projections descending from the reticular formation and some connections coming from the hypothalamus are assigned to these manifestations that accompany the fluctuating of consciousness, and consist of bundles of fibers that come from the motor structures of the trunk.

- c. *Electrical activity of the brain*, which is the expression of the functional level of the cerebral cortex: the ascending reticular projections are responsible for the vigilance level and modulation of the cerebral electrical activity.
- d. *Contents of consciousness*, as the sum of mental activities (perceptions, thoughts, feelings, dream activity, etc.) that occupy the mind at any given time. The cerebral cortex is the seat of mental activities and content of consciousness. In general, cortical areas can be schematically divided into two types, specific and associative. The specific areas deal with elementary functions, such as the reception of sensory information or the execution of a movement. Associative areas establish connections between the different portions of the cortex and perform integrative functions: for example, they process sensory information and are responsible for the recognition of objects or the development of motor strategies.
- e. *Self memory*, that is the continuous comparison between coming sensory experiences, past experiences and the perception of one's own identity. The hippocampus, the medial temporal cortex and the sensory associative areas are responsible for the storage and retrieval of memories. The associative cortex houses both short-term and long-term memory.
- f. *Selective attention*, which is the concentration of mental activity on a certain content. It can be the unconscious result of a meaningful stimulus or the voluntary choice of a field of interest, such as the face of a person known in the crowd or a mathematical problem to be solved. Posterior parietal, basal temporal and prefrontal associative cortical zones are responsible for selective attention. When a stimulus with a high quotient of interest is collected by the sense organs, the information is transmitted to specific cortical areas and, through the circuits of memory, compared with past experiences and deposited in the areas of storage of memories. [3]

1.3 Levels of consciousness

To date, it's far from clear what precisely a level of consciousness is supposed to be. Consciousness is typically taken to have two aspects: **local states** and **global states**. Local states of consciousness, also called 'conscious contents', include perceptual experiences of various kinds, imagery experiences, bodily sensations, affective experiences, and occurrent thoughts, typically distinguished from each other on the basis of the objects and features that they represent. By contrast, global states of consciousness are typically distinguished from each other on cognitive, behavioural, and physiological grounds. For example, the global state associated with alert wakefulness is distinguished from the global states associated with

post-comatose conditions or with light-to-moderate degrees of sedation, dreaming, hypnosis, and epileptic absence seizures.

The term “level of consciousness” is employed to describe the global states of consciousness and it derives from the clinical literature on disorders of consciousness. Recently, the integration of clinical and theoretical approaches to consciousness led to a new measure of levels of consciousness, the **Perturbational Complexity Index** (PCI).

As Figure 1.1 shows, the PCI is designed to explain the classic distinction between level and content of consciousness, starting respectively from the concepts of wakefulness and awareness.

- *Wakefulness* is characterized by a state of vigilance that may not be associated with awareness of what is happening in the surrounding world.
- *Awareness* consists in having cognition of the surrounding world and of one’s being.

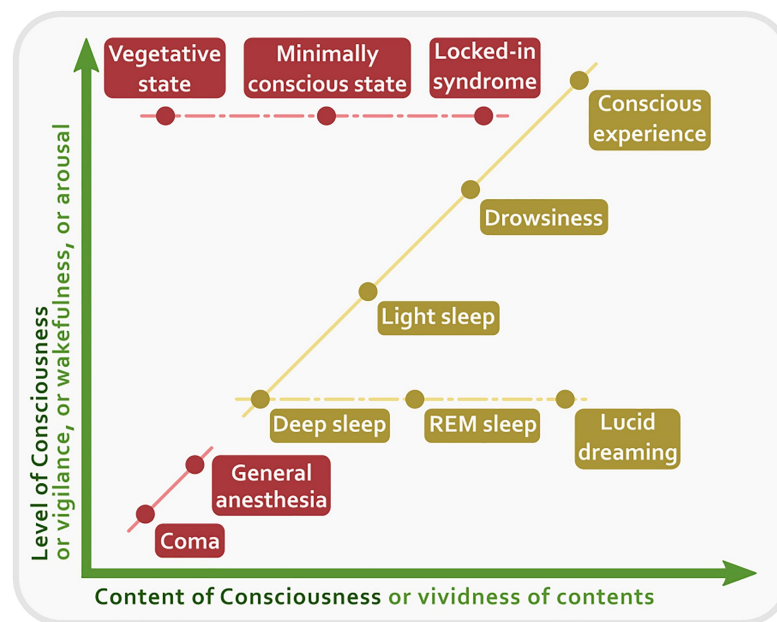


Figure 1.1: A two-dimensional representation of consciousness. The X axis represents the Content of Consciousness, the experience of which can vary in vividness. The Y axis represents the Level of Consciousness, or wakefulness, or vigilance, or arousal. Clinical conditions are in red, while normal physiological states are in yellow.

The PCI was introduced by Casali et al. (2013) and tested on TMS-evoked potentials measured with EEG: using PCI, they were able to discriminate levels of

consciousness during wakefulness, sleep, and anesthesia, as well as in patients who had emerged from coma and recovered a minimal level of consciousness. [4]

1.3.1 Disorders of consciousness

Brain lesions that disturb consciousness affect one or more of the following four structures: reticular formation, reticular-thalamic-cortical pathways, cerebral cortex, and memory circuits.

Disorders of consciousness include coma (cannot be aroused, eyes remain closed), vegetative state (can appear to be awake, but unable to purposefully interact) and minimally conscious state (minimal but definite awareness). Locked-in syndrome is not a disorder of consciousness, but can look like one because of paralysis of limbs and facial muscles that causes an inability to speak and/or appearance of being unable to react.

- **COMA** is the non-responsiveness from which the patient cannot be awakened. The person in a coma is in a state of unconsciousness and is not able to follow simple orders (open the eyes, pronounce understandable words) but can partially or totally preserve vegetative functions (blood circulation, breathing, etc.). The state of coma occurs when there is a disruption of nerve impulses between the cerebral cortex (gray matter) and neurons located in the brain stem. The condition of coma usually does not last longer than 4 weeks, after which patients either evolve to brain death (i.e., permanent loss of brainstem functions) or may completely recover consciousness or evolve to a vegetative state (VS). [5, 6]

The signs and symptoms of a coma commonly include:

- closed eyes;
 - depressed brain stem reflexes, such as pupils that do not respond to light;
 - no response to environmental stimuli (sound, light, pain) except for reflex movements;
 - irregular breathing;
 - inability to communicate;
 - reduction of the basic reflexes (cough, swallowing, breathing).
- **VEGETATIVE STATE (VS)** is characterized by the absence of responsiveness and consciousness due to severe dysfunction of the cerebral hemispheres, with sufficient savings of the diencephalus and the brain stem such as to preserve the neurovegetative and motor reflexes and the normal sleep-wake cycle.

Patients in a vegetative state show no signs of awareness of themselves or the environment and cannot interact with others. [7]

Typical manifestations of the vegetative state can be:

- inability to react to the visual threat and to execute orders;
 - faecal and urinary incontinence;
 - limbs can move, but the only finalistic motor responses that stand out are primitive (e.g. grabbing an object that comes into contact with the hand);
 - pain usually causes a motor response, but not a voluntary avoidance response;
 - cranial nerves and spinal reflexes are typically preserved.
- **MINIMALLY CONSCIOUS STATE (MCS)** is a condition of severely altered consciousness in which minimal but definite behavioral evidence of self or environmental awareness is demonstrated.
MCS is distinguished from VS by the presence of behaviors associated with conscious awareness. In MCS, cognitively mediated behavior occurs inconsistently, but is reproducible or sustained long enough to be differentiated from reflexive behavior.
MCS may occur after a coma or may represent the evolution of a previous vegetative state; it may be present for a short period or may last for a more or less protracted or indefinite time until the patient's death.[8]
 - **LOCKED-IN SYNDROME (LIS)** is a state of vigilance and awareness accompanied by tetraplegia and paralysis of the last cranial nerves that results in the inability to change facial expression, move, speak or communicate, except through codified eye movements.
It's like the patient is paralyzed in his own body: patients have full cognitive function and are awake, they can hear and see, with eyes open and a normal sleep-wake cycle. In order to functionally communicate, it is necessary for the LIS patient to be motivated and to be able to receive (verbally or visually) and emit information. The only contact with these patients is through a code, using eyelid blinks or vertical eye movements.[9]

1.3.2 Behavioural assessment methods

Because of the difficulties in the definition of a patient's degree of consciousness, assessment scales have been developed for helping doctors with a primitive and quick diagnosis. The behavioral examination is the "gold standard" for detecting symptoms of consciousness in severely brain-injured patients [10].

- **Glasgow Coma Scale (GCS)**

The scale assesses patients according to three aspects of responsiveness: eye-opening, motor, and verbal responses.

The levels of response in the components of the Glasgow Coma Scale are 'scored' from 1, for no response, up to normal values of 4 (Eye-opening response), 5 (Verbal response) and 6 (Motor response).

Changes in motor response are the predominant factor in more severely impaired patients, whereas eye and verbal are more useful in lesser degrees.

The total Coma Score has values between 3 (deep unconscious state) and 15 (maximum conscious state).[11]

- **AVPU**

This scale is based on neurological assessment through the patient's response to the external stimuli induced by the rescuer, as it is used especially in the first aid out of hospital.

AVPU is an acronym for Alert, Verbal, Pain, Unresponsive: each letter identifies a different stage of consciousness based on the type of stimulus needed to evoke a response from the patient. [12]

- **Alert:** the patient is awake and conscious; this state is evaluated positively if the patient can respond clearly to simple questions such as "What happened?" or "What's your name?".
- **Verbal:** the patient also responds by moving the eyes or by acts motor but only to verbal stimuli, without stimuli is confused or drowsy.
- **Pain:** The patient only responds to painful stimuli, for example shaking (in the patient not traumatized) and/ or pinching the neck base.
- **Unresponsive:** patient does not respond to verbal or painful stimuli and is therefore completely unconscious.

- **Wessex Head Injury Matrix (WHIM)**

This scale was created to observe cognitive functions during rehabilitation after severe brain damage. The scale consists of a sequence of 58 observable parameters on communication skills, cognitive skills and social interaction. Parameters are encoded with a number that corresponds to an increasing degree of difficulty of the action: from "Eyes open briefly" (number 1) to "Remembers something from earlier in the day" (number 57). The test starts with basic attention parameters and proceeds by confirming with a tick or marking as unavailable with a cross. After ten crosses in a row have been made, the examination is finished. The value WHIM is the highest number of observed values.[13]

1.3.3 Instrumental assessment methods

The clinical assessment of a patient's state of consciousness is often the result of behavioural observations combined with the patient's clinical history. Sometimes, especially in the most severe cases of patients with DOCs, behavioural analysis is not so accurate, as different situations may occur:

- a) the patient may be unable to speak or move;
- b) the subject may have a so altered state of consciousness that it produces inconsistent or incomplete behaviour;
- c) the motor response may be undetectable or not produce an obvious output.

Over the years, these situations have led to misdiagnoses of VS, MCS and LIS, because responsiveness represents only an indirect evidence of consciousness. The main causes of misdiagnosis are associated with patient's disabilities, such as paralysis and aphasia, fluctuation in arousal level, difficulty differentiating between reflexive and voluntary movements or the presence of drugs' side effects.

It was necessary to reduce clinical errors and overcome the limits of behavioral assessment in the detection of possible retained consciousness in unresponsive patients, also because the definition of a subject's state of consciousness raises important ethical and medical issues, including end-of-life decision and pain treatment.[6]

A **multimodal approach** for the definition of a subject's state of consciousness has been developed: behavioral analysis can be supported by *functional neuroimaging techniques*, such as PET, fMRI, TMS and DTI, *electrophysiological methods*, analyzing EEG signals and Event Related Potentials (ERP).

The technology-based assessment of the level of consciousness relies on information obtained by combining the temporal and spatial properties of different techniques: the brain's metabolic capacities (with PET), its hemodynamic function (with fMRI), the metabolic and biochemical activity (with MRI spectroscopy), its structural properties (with diffusion weighted MRI), and the dynamics of cortical excitability (with EEG recordings after transcranial magnetic stimulation).

A brief overview of instrumental assessment methods will follow, which help in highlighting the underlying pathophysiology of disorders of consciousness.

- **Positron Emission Tomography (PET)**

Positron emission tomography (PET) is a nuclear medical imaging technique for assessing brain activity and function by recording the emission of positrons from radioactively labeled molecules. If the chosen molecule is fludeoxyglucose (FDG), an analogue of glucose, the concentrations of tracer imaged will

indicate tissue metabolic activity by virtue of the regional glucose uptake and hence neural activity.

In comatose patients, PET studies showed on average a reduced grey-matter metabolism up to 50-70 % of normal range in patients of traumatic or hypoxic origin. Global cerebral metabolism was shown to correlate poorly with the level of consciousness, as measured by the Glasgow Coma Scale: a global decrease in cerebral metabolism, in fact, is not unique to coma, as it can be associated to several different situations with temporary loss of consciousness, such as deep sleep, general anesthesia and Cotard's syndrome.

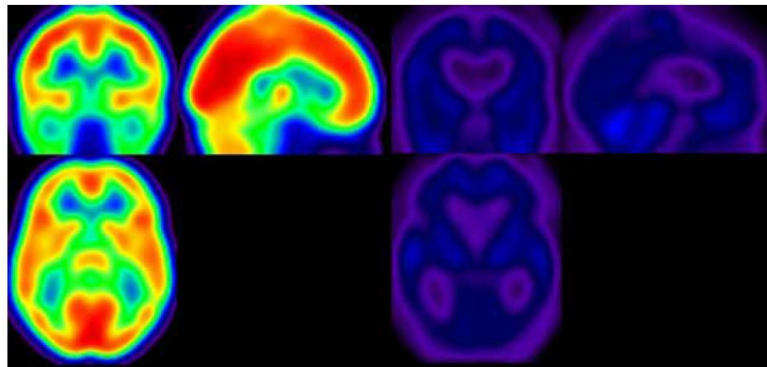


Figure 1.2: Global brain metabolism detected by FDG-PET in a healthy control (left) and in a patient in an unresponsive wakefulness syndrome (right). Red colorscale indicates regions with high consumption of glucose; blue colorscale indicates regions with low consumption of glucose.[6]

In VS or MCS, where awareness is impaired whilst wakefulness is spared, PET studies showed that unresponsive patients are characterized by reduced global metabolism compared with healthy subjects. PET studies using passive auditory and noxious stimulation have furthermore demonstrated a peculiar disconnection in VS/MCS patients between the primary sensory areas and these large-scale associative fronto-parietal cortices, which are thought to be required for conscious perception. In line with their clinical condition, patients in MCS show a partial preservation of this large-scale associative fronto-parietal network. As Figure 1.2 shows, in terms of diagnostic accuracy, cerebral metabolic information obtained by PET has shown to be able to specifically and reliably differentiate VS/MCS from LIS patients and healthy controls. [6]

- **Functional Magnetic Resonance Imaging (fMRI)**

Functional magnetic resonance imaging (fMRI) measures brain activity by

detecting changes associated with cerebral blood flow, since it increases when an area of the brain is in use. It relies on the natural diamagnetic properties of oxygenated hemoglobin and paramagnetic properties of deoxygenated hemoglobin and it correlates the cerebral blood oxygenation with neural activity. In the last decade, fMRI has been largely used in patients with DOC in order to detect brain activity related to residual cognition and awareness, and in some cases even established two-way communication, without requiring any behavioral output from patients. [6]

However, it is becoming increasingly apparent that some patients have undetectable cognitive abilities, as the peripheral motor system is damaged. Laureys et al. conducted recent studies that highlight the importance of neurofunctional imaging in the identification of these residual cognitive functions, proving that patterns of brain activation can be found without a willful intervention on the part of the participant after many types of stimuli (e.g. faces, speech, pain) even in cases where the patient has been diagnosed as VS with behavioural assessments: that means that the patient does not respond to commands and stimuli because of his motor impairment and not because he fails to receive and process them.[14] As can be seen from the studies mentioned in the following lines, the imagined action plays a fundamental role in the identification of a state of consciousness.

Owen et al. conducted a recent fMRI study using mental imagery tasks (imagining playing tennis vs. spatial navigation around one's house) in a large cohort of 54 patients with DOCs. Despite the majority of them had been diagnosed VS/MCS with behavioural assessments, five patients showed the ability to understand spoken commands and to respond to them through brain activity rather than through speech or movement.

Imagery tasks elicited distinguishable patterns of activation in specific regions of the brain, that have been compared with the results of studies in healthy volunteers doing the same tasks: imagining playing tennis elicits activity in the supplementary motor area, a region that houses imagination, while imagining moving from room to room in a house commonly activates the parahippocampal cortices, the posterior parietal lobe, and the lateral premotor cortices, regions that contribute to imaginary or real spatial navigation.[15, 14]

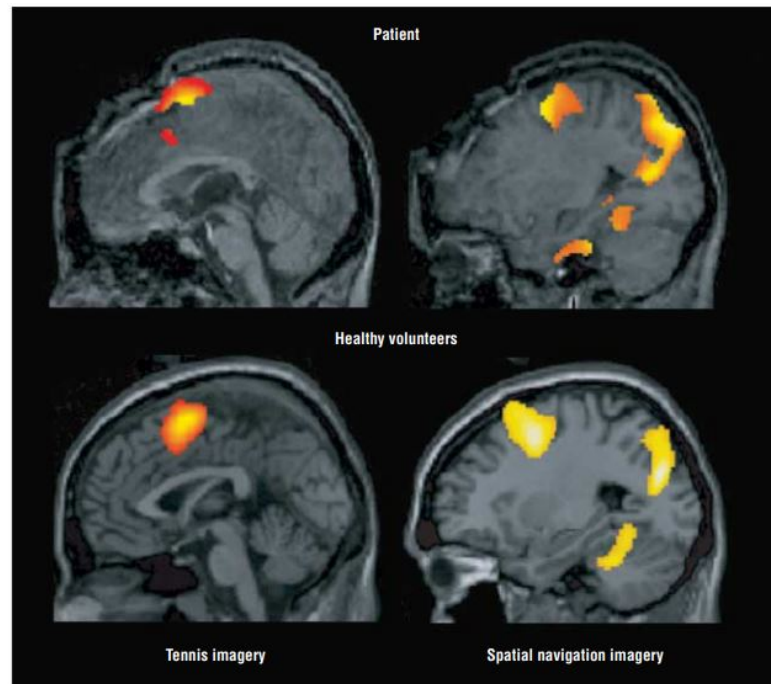


Figure 1.3: Supplementary motor area activity during tennis imagery in a patient diagnosed as being in a vegetative state and in a healthy volunteer (left). Parahippocampal gyrus, posterior parietal lobe, and lateral premotor cortex activity while imagining moving around a house in the patient and in a healthy volunteer (right).[14]

These results (Figure 1.3) provide further evidence that some vegetative patients retain islands of preserved function and that in the absence of behavioural evidence, functional imaging provides a valuable tool to the assessment team.

- **Diffusion Tensor Imaging (DTI)**

Diffusion tensor imaging (DTI) derives from diffusion weighted imaging which uses the diffusion of water molecules to generate contrast in MR images. Although white matter looks rather homogenous, it consists of axonal bundles with complicated architectures: in the brain, water molecules do not move freely, but there is a number of biological barriers depending on tissue organization. Because of this restricted motion, the diffusion of water protons follows a preferred direction: it is higher along fiber tracts than across them in the white matter, which allows for directional measurement of diffusion and, hence, measurement of structural integrity.

DTI data can be used to compute the fractional anisotropic index, which quantifies anisotropic diffusion in the brain, related to the density, integrity,

directionality and crossings of white matter tracts. DTI provides anatomical features and details about the architectural organization of white matter fibers that can only be seen by performing histological examination: the advantage is the possibility of using it for in vivo detection of diffuse axonal injury after brain trauma, even in sedated patients. [6]

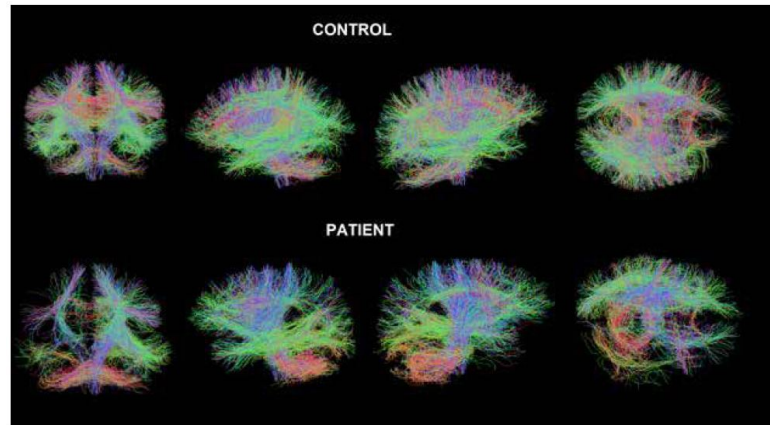


Figure 1.4: Neural tracks obtained with DTI in a healthy control (top) and a patient in MCS (bottom) confirms the structural damage which is evident in the temporo-parietal regions of the right hemisphere (bottom right - T1 MRI structural image). Colors indicate directionality of water diffusion: red = left-right; green = anterior-posterior; blue = superior-inferior.[6]

Several studies have been carried out on traumatic brain injured (TBI) patients using DTI to assess the level of damage and comparing the results with the scores obtained with the behavioural assessment.

Recent studies on TBI patients and anoxic patients that underwent cardiac arrest have shown that quantitative DTI increases the accuracy of long-term outcome prediction compared with the available clinical or radiographic prognostic score in both cases.

In a study conducted by Fernandez-Espejo et al., DTI has been used as an in vivo technique for distinguishing VS patients and MSC patients in a group of 25 TBI subjects, both from the diagnostic and etiologic point of view: the MCS and unresponsive patients differed significantly in subcortical white matter and thalamic regions, but appeared not to differ in the brainstem. DTI results has been compared with the predicted behavioural scores, and it revealed a successful classification of the appropriate category with an accuracy of 95%. Furthermore, DTI showed to be helpful for characterizing etiologic differences in patients in VS/UWS.[16]

DTI has proven to be an excellent biomarker for consciousness recovery after a traumatic brain injury, as an objective method for early classification of injured patients to complement the behavioural assessment.

- **Electroencephalography and Transcranial Magnetic Stimulation (EEG-TMS)**

Electroencephalography (EEG) recordings play an important role in the assessment of DOCs in severe brain injured patients, whether it is of traumatic or anoxic origin. In both cases, the EEG can be altered and display abnormalities, which mainly occur as a slowing of the brain activity: the predominant rhythm is no longer posterior alpha (related to the awake stages in adult healthy individuals) but diffuse theta or delta (normally present in the slow stages of sleep in healthy adult individuals).

However, standard EEG recordings can solely offer a first global view of the cerebral activity and function, but this technique cannot be used alone in order to obtain an accurate diagnosis, since the patterns are not specific of the aetiology and the same subject can have varying patterns in short intervals. Furthermore, the outcome does not depend uniquely on the brain affection itself, but on the overall condition of the patient: the capacity of a patient to follow commands is a critical diagnostic marker in DOC, but there are several reasons for which it may be compromised, not only due to brain injury but also for damage to the peripheral motor system.

In this perspective, active paradigms are designed (i.e. mental imagery during EEG), in order to quantify the patient's engagement in the mental task by his/her ability to generate reliable, temporally and/or spatially specific modulation of brain activity. Since these protocols may have produced false positive results due to the random nature of EEG artifacts in patients, alternative methods were developed. [17]

As already mentioned, an atypical pattern in the EEG recording does not necessarily imply the lack of consciousness. For this reason, an alternative solution has been explored: EEG combined with *Transcranial Magnetic Stimulation (TMS)*, useful in the consciousness assessment because it does not rely on a subject's ability to process sensory stimuli, to understand and follow instructions or to communicate.

TMS is non-invasive stimulation technique that uses electromagnetic induction to generate an electric current across the scalp and skull. Pulsed current is discharged through a coil without physical contact, stimulating a subset of cortical neurons and modulating neural activity within the cerebral cortex. EEG recordings support TMS in order to measure the effects produced by this perturbation in the rest of the brain. For patients in VS, TMS either

induced no response or triggered a simple, local EEG response, indicating a breakdown of effective connectivity similar to the one observed in deep sleep and anesthesia. For patients in MCS, instead, TMS triggered complex EEG activations that sequentially involved distant cortical areas, similar to activations recorded in patients in LIS and healthy awake subjects, even though no conscious behaviour could be observed.

TMS-EEG seems to be a promising technique in the assessment of DOC patients, because it is handy, not invasive and it does not require patients' cooperation.[6]

Chapter 2

Consciousness measurement: EEG signal and Movement-Related Cortical Potentials (MRCP)

As previously seen, the definition of consciousness and levels of consciousness is a challenging topic that needs to be improved.

From the diagnostic point of view, behavioural assessments can provide general and summary information on the patient's state of consciousness, based on evidence found in attitudes and responses, voluntary and not. Nevertheless, this type of assessment can lead to a large number of misdiagnoses or inaccurate diagnoses, depending on the severity of brain injury, which may reveal incomplete or inconsistent behaviours.

For this reason, behavioural assessments must be integrated with neurofunctional imaging, which allows an objective assessment that overcomes the limits of behavioural evaluation in the detection of possible retained consciousness in non-responsive patients. Particularly to explore cognitive function in unresponsive patients through a reproducible motor command, this project's aim is the implementation of a Brain Computer Interface (BCI), a non-invasive technology that allows its user to deliver mental commands to a robot controller that transforms them into appropriate motor actions.

As many studies confirm, consciousness is closely linked to the volitional movement, whether it is actually accomplished or just imagined, and intention is meant as the time of awareness of wanting to perform a reaching task.

An ERP component linked to intentional movement is Readiness Potential (RP), on which the study of this thesis is based, to better understand its contribution during voluntary, semi-voluntary and involuntary movements acquired by electromyography (EMG), according to an experimental protocol. Readiness Potentials have been found to be modulated by the consequence of movement, complexity of the movement, level of skill, sequence of hand movements, the part of the body performing the movement, force, speed, and precision of a movement. Starting from EEG recordings, indeed, the focus on Readiness Potentials can be useful for two reasons:

- The classification of voluntary, semi-voluntary and non-voluntary movements, that can help in the definition of the patient's state of consciousness.
- The localization of motor control after brain lesions, in order to draw up an accurate rehabilitation protocol and follow motor functional improvements.[18]

2.1 Biosignals: Electroencephalography and Electromyography

This project's development required the use and recording of two fundamental biological signals, the electroencephalographic (EEG) signal and the electromyographic (EMG) signal, in order to analyze the correlation between intention, consciousness and movement.

Here is a brief overview of this two types of biological potential: their morphological characteristics over time and frequency, how they are generated and how they are recorded.

2.1.1 EEG signals

Electroencephalography is a technique that relies on the acquisition of brain potentials corresponding to various states (sleep, wakefulness, anesthesia or death), that reflect human cognitive behaviour. Human behaviour can be analysed in terms of attention, motor reaction, remembrance and concentration, related to a specific signal range of frequencies.

Neurons act like information carriers between human body and brain: EEG signals are almost exclusively produced by post-synaptic potentials, that are potentials arising in the target cell due to the electrochemical mediation of the neurotransmitter, released by the pre-synaptic neuron. Post-synaptic potentials are easier to record with respect to action potentials for two main reasons:

- a. the amplitude of the field produced by an action potential decreases much faster than the amplitude of the field produced by a post-synaptic potential;

- b. the duration of the action potentials is very short and producing a non-invasive recordable activity requires a high level of synchronization between the different pyramidal neurons, to make possible a space-temporal summation able to create detectable differences of electric and magnetic fields.

EEG signals are acquired with a special device, the electroencephalogram, comprised of electrodes, used for conducting electrical activity from the scalp, conductive gel, amplifiers and Analog-to-Digital converters. The electrodes, often reusable, are placed on the scalp with a small amount of conductive gel (Ag-Cl): multiple electrodes are organized on a cap, in order to record different signals coming from different areas of the skull (Figure 2.1).[19]



Figure 2.1: EEG cap for brain potentials recordings.

Electrodes are arranged according to 10-20 standards for EEG placement, as shown in Figure 2.2, which indicates the position and the label of the electrode relying on the distance from particular landmarks (ears, nasion or inion). Each electrode is named with letters for the brain lobes (F-Frontal, T-Temporal, C-Central, P-Parietal and O-Occipital lobe) and numbers indicating the hemisphere (odd-left and even-right). Electrodes are positioned in order to acquire all the most significant signals with respect to the main functions of the brain, such as sensory and motor function (Central lobe), cognitive processing (Parietal electrodes), emotional and verbal memory (Temporal lobe), visual processing stimuli (Occipital zone), intention and motor planning activities (Frontal lobe), intention and judgement impulse (Fp line).

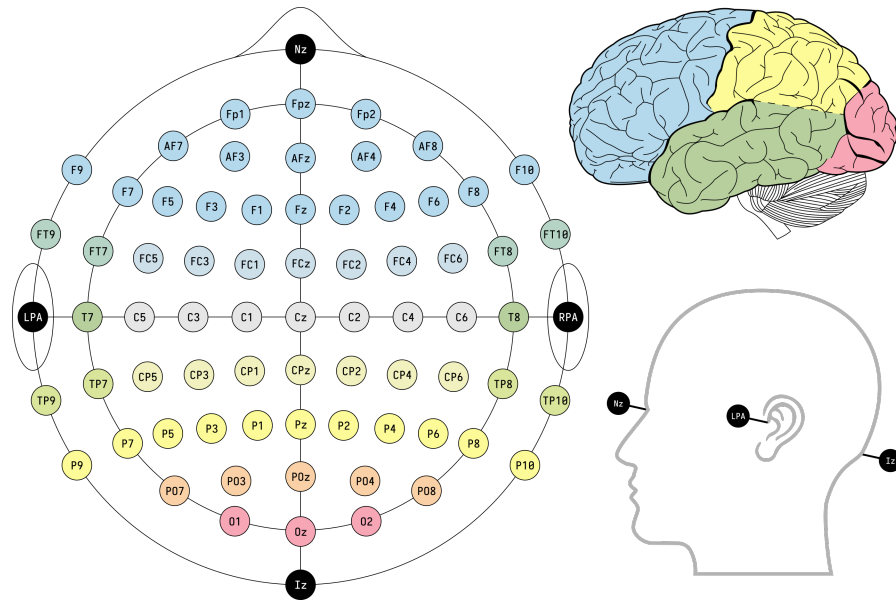


Figure 2.2: International Standard 10-20 for electrodes setup in EEG recordings.

EEG waveforms are distinguished by their amplitude, variable between 10 and 500 μV , morphology, topography, symmetry and synchrony. Abnormal or pathological rhythms are determined by the classification of EEG signals according to their frequency: in fact, different frequency bands have been identified, common from subject to subject, and corresponding to different behaviours and mental states of the brain [19]. In particular:

- *Delta waves (0.1-4 Hz)*
These waves have low frequency but the highest amplitude, due to the strong synchronization of neurons in generating cortical potentials. They are found in deep sleep, infants and comatose patients.
- *Theta waves (4-8 Hz)*
Related to subconscious activity, they are observed in deep relaxation and meditation. Abnormal in adults but normal in children under 13 years, they encourage the production of serotonin, which increase relaxation and get relief from pain, and cortisol hormone, that helps for memory and learning.
- *Alpha waves (8-14 Hz)*
Normal in adults while mental relaxed with closed eyes, they occur on both sides of the head but have higher amplitude in non-dominant side: they act like a bridge between conscious and subconscious state.
- *Beta waves (13-30 Hz)*
Related to thinking and conscious actions, these waves indicate an activation

of the cortical areas and they occur with talking, problem solving, judgement, decision making, that all require attention and concentration.

- *Gamma waves (30-100 Hz)*

Associated with perception and full awareness, these waves are found during hyper alertness and integration of sensory inputs, combining sensory experience and memory.

- *Mu waves*

EEG signal waves observed in the frequency band between 7.5 and 12.5 Hz, they only come from the motor cortex and are suppressed when a movement is made or there is the intention. They are used in Brain Computer Interfaces for the design of devices reproducing the movement, receiving the intention from the absence of mu waves in the EEG path.

- *K-Complex*

This kind of wave occur in a run of theta waves with high amplitude, often after a sensorial stimulus during deep sleep.

- *Lambda waves*

They occur during visual exploration, when the person stares at blank surface or reads or watches television.

- *Spike waves*

These waveforms are seen mostly in children, usually in the delta waves range of frequency. They may occur synchronously in epilepsy and more usually with brain injury.

- *Sleep Spindles*

Also called “sigma activity”, it is seen in 11-15 Hz range of frequency and it occurs during deep sleep, as markers of the slowing in the frequency content.

2.1.2 EMG signals

Electromyography (EMG) is a technique for measuring muscle response or electrical activity after a nerve’s stimulation of the muscle, using a specific instrument called electromyograph.

Generally, in a resting state, muscles do not produce electrical signals: when a stimulus occur, a brief and wide signal may appear, but after that, no signal should be present.

The EMG signal can be obtained either by voluntary contractions, following a neurological activation of the muscle fibers, or by electrically stimulated contractions: in the first case, a random signal can be observed, in the second case, a

deterministic signal may come out.

The muscle's functional unit is the motor unit (MU): it's the set of the alpha motor neuron and the muscle fibers that it innervates (Figure 2.3).

Each muscle fiber consists of two proteins, actin and myosin, which slip between them: in resting conditions, they are arranged parallel to each other, while when the fibers are in contraction, the proteins overlap, giving rise to a geometric deformation of the muscle and producing a torque effect that, through the tendons, is discharged on the joint.

From the spinal cord depart several axons belonging to the motor neurons: under normal conditions, an action potential propagates through the axons that activate all the muscle fibers of the motor unit. When the post-synaptic membrane of the muscle fiber is depolarized, such depolarization propagates in both directions, obtaining different waveforms depending on the placement of the electrodes. The depolarized membrane, accompanied by a movement of ions, generates a magnetic field in the vicinity of muscle fibers. An electrode located in this field will detect the potential, whose temporal excursion is known as action potential.[20]

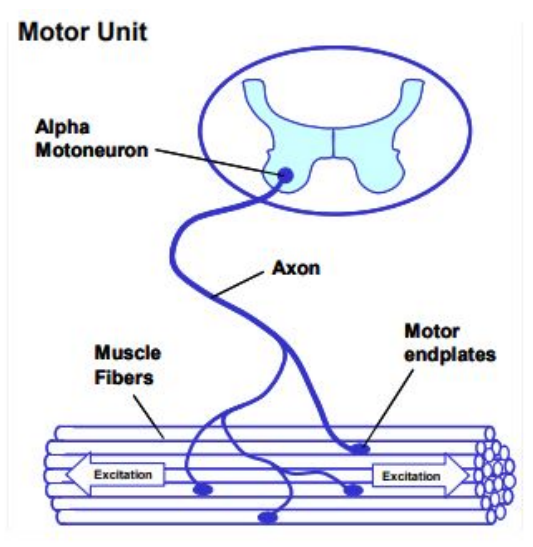


Figure 2.3: Motor Unit (MU) and its innervation.

The resulting signal is the space-time summation of the individual action potentials produced by the depolarization of the muscle fibers of a motor unit, and it is called MUAP (*Motor Unit Action Potential*), and depends on the geometric arrangement of the electrodes, the filter functions of tissues and electrodes and the degree of synchronization of the action potentials (Figure 2.4).

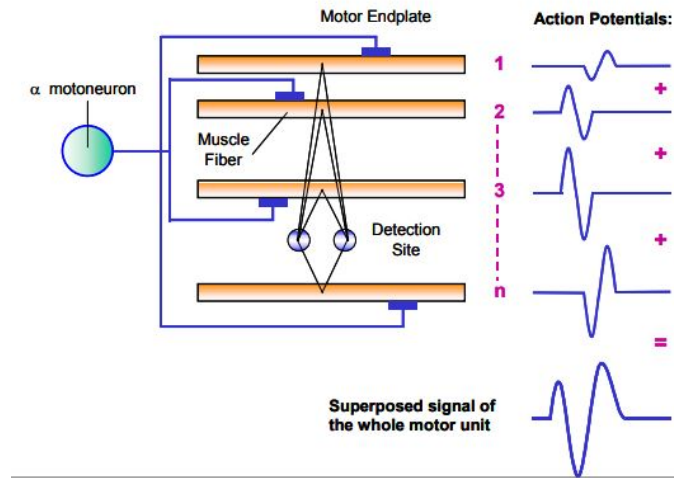


Figure 2.4: Motor Unit Action Potential (MUAP) resulting from the summation of fibers' action potentials: with the same motor task, it changes width and shape in dependence on positioning of the electrode compared to the fiber of MU.

In the electrode detection zone, there are contributions from other motor units, so a series of MUAPs are detected. These can have similar amplitude and shape, if each muscle fiber belonging to the respective motor unit has the same distance from the detection zone. The resulting MUAPs sequence is called MUAPT (*Motor Unit Action Potential Train*). Since the MUAPTs of the individual motor units are not synchronous, their summation leads to a surface electromyographic signal, called "interference signal", which is added to the noise caused by the interfacing of the biological world with the electronic system: by filtering the overall signal with the transfer function of the recording system, the EMG signal is obtained.[20]

EMG signals are mainly recorded in two different ways:

- **Surface EMG**, used for the EMG recordings of this study, it is a non-invasive technique that uses a pair of electrodes or a more complex array of multiple electrodes in order to recording muscle activity from the surface above the muscle on the skin. The resulting signal is the potential difference between two separated electrodes, so more than one electrode is needed. Some limitation of this approach can be highlighted: a) because of the large volume of the subtended tissue, a small Signal-to-Noise ratio is probable to occur; b) the adipose tissue between the skin and the muscle acts like a low-pass filter, resulting in a lower frequency band signal (250-300 Hz) with respect to more invasive techniques; c) recordings are restricted to superficial muscles, so the

behaviour of the deepest fibers cannot be elicited.[20, 21]

- **Intramuscular EMG**, an invasive technique that records muscles electrical activity inside the sourced that generate it. A variety of different types of recording electrodes is used: the simplest approach is a monopolar needle electrode, a fine wire inserted into a muscle with a surface electrode as a reference. Normal muscles exhibit a brief burst of muscle fiber activation when stimulated by needle movement, but this rarely lasts more than 100ms. Limitations of this approach are pain for the patient, sterility and disinfection, but it allow for the signals of individual muscle fibers to be discriminated.[20, 21]



Figure 2.5: Surface EMG electrodes.



Figure 2.6: Intramuscular EMG recordings.

In the case of voluntary contractions, in addition to geometric variations (reciprocal position of the electrodes with respect to the signal) and external noise due to coupling with other electromagnetic sources, the EMG signal is affected mainly by two different factors[21]:

- *The firing rate*, that is the interval between two consecutive discharges of the same MU: if a muscle fiber is stimulated repeatedly at short intervals of time, it will result in a fusion of the individual shocks, to form a continuous contraction called "muscle tetanus", far greater than that of the single shock. It is determined by the operating conditions required to perform a task, such as the duration and extent of muscle contraction, and it is irregular, such that it can be considered a random variable;

- *The recruitment of MU*, which determines the amount and type of muscle fibers recalled and establishes the intensity of work and the synchronism of the fibers themselves based on the level of force required.

2.2 Conscious intention and motor cognition

From the neurological point of view, it has been demonstrated that the state of consciousness, understood as awareness of oneself and of the surrounding world, is closely related to the concepts of free will and motor intention, regardless of whether the action is then actually performed or just imagined (Libet B.,1977). Being aware of one's own actions and the fact that they can be controlled is a fundamental aspect of conscious experience, but it is necessary to make distinctions between some fundamental concepts:

1. *Intention of the movement*: one decides to move, one wants to move (present only in voluntary movements);
2. *Consciousness of the intention*: one is aware that he/she has decided to move;
3. *Consciousness of the movement in progress*: one knows that he/she is moving;
4. *Consciousness to have completed the programmed movement*: one knows that he/she has moved carrying out the action that he/she wanted.

The sequence of neurobiological events that leads to the fulfilment of an action involves some cognitive stages, not always aware, aimed to implement the motor intention.

Many studies have long focused their attention on the conscious intention and motor cognition: as Patrick Haggard, professor of neuroscience at University College London, affirms, a voluntary movement requires a stage of motor preparation, totally unaware, which precedes the "conscious intention", which carries out the activity of deciding whether to carry on the action or to place a veto.[22]

The consciousness of the motor intention activates the front of the pre-supplementary motor area (SMA) and it is independent on the execution of the movement (Figure 2.7): while damages to the motor cortex and the descending nerve pathways cause more or less complete paralysis of the extremities contralateral to the injury, damage to premotor areas such as SMA and parietal areas can produce more complex deficits of motor cognition, which also alter awareness and intentionality.

This conclusion elicits that the awareness of the movement is unrelated from the neurosensory feedback that comes from the execution of the movement, but it is closely related to the programming of the movement itself, so the phases of motor preparation and conscious intention of the action.

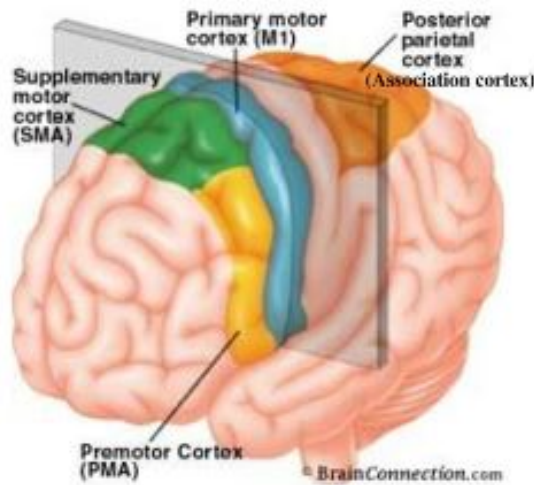


Figure 2.7: Cortical areas involved in voluntary motor control.

Blakemore, Wolpert and Frith have developed a model that reproduces the sequence of events that trigger in the brain before the execution of the movement, assuming that, together with the programming of the motor action, a prediction of the consequences of the movement is also produced, on which motor awareness is built (Figure 2.8). [22, 23]

Starting from the *desired state*, the model consists of four basic blocks:

- i. **Motor planner**, which generates the motor commands relying on the difference between the *actual state* and the *desired state*. It converts the desired state into a sequence of motor engrams needed to achieve it, of which two copies are created: the first copy is intended for the motor cortex, responsible for the realization of the movement, the second copy, called "*efferent copy*" is intended for the predictor, the next block.
- ii. **Forward model**, that for each movement programmed by the motor programming system, estimates the sensory consequences of the implementation of the movement (predicted state). The prediction is formed after the sending of the motor commands, from which it analyzes the engrams, but before the execution of the movement.
- iii. **Comparator A**, which compares the *desired state* with the *predicted state*, provided by the forward model: if they coincide, the subject gets the "sense of agency", as the perception of performing the movement, which is manifested before the execution of the movement itself.
- iv. **Comparator B**, which compares the *predicted state* and the *implemented state*, after the movement, integrating information from the environment and sense

organs: if the states coincide, the subject has the awareness of a movement that has actually been performed. Studies by Berti et al. have shown that damage to the comparator B can lead to disorders such as *anosognosia for hemiplegia* (which will be investigated later), a transient condition of some hemiplegic subjects, in which the patient is not aware of the paralysis of which he is affected, he openly claims not to have any problems and to be able to move correctly both the paralyzed arm or leg. These subjects, in fact, preserve both the intention and the planning-prediction of the movement, therefore the sense of agency generated by the comparator A, but they do not possess the awareness of the executed or not executed movement, dictated by the comparison between planned and implemented state, deputed to the comparator B.

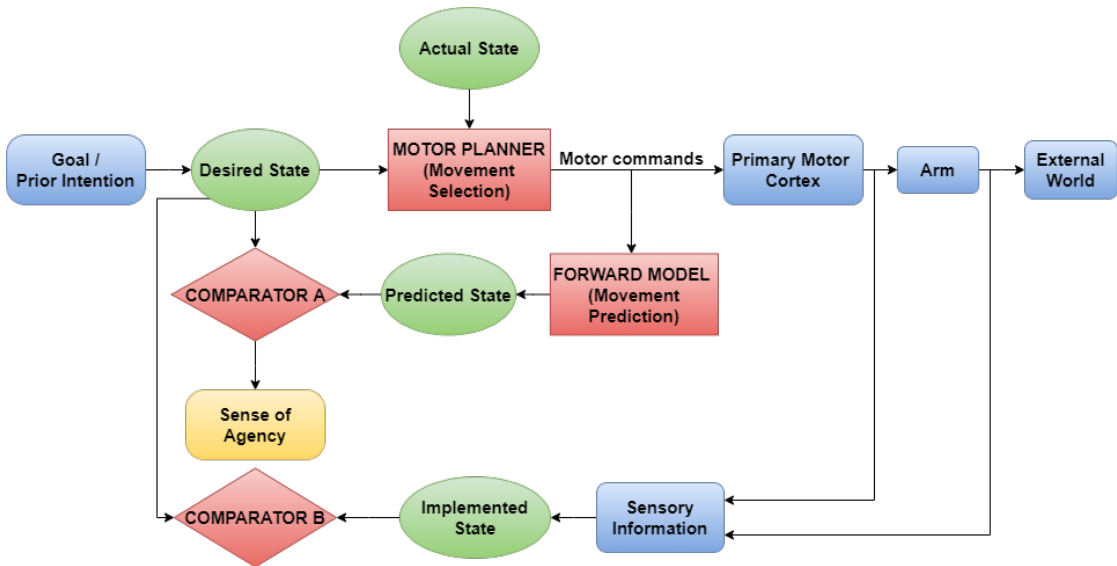


Figure 2.8: Computational model for movement execution. Red blocks provide movement selection and prediction, conscious intention and awareness of the action.

This model highlights how motor cognition is linked to the conscious intention to carry out the movement and to the sense that actions cause effects in the external world (the so-called "agency").

Many philosophers and scientists have debated about conscious intention that might cause action, but in the last decades, the idea of the mind-body causation has been rejected: many findings suggest that conscious experiences are consequences of brain activity, rather than causes.[22] Recently, what the scientists focus on is the idea that there is a preparatory, totally unconscious, activity of the brain that occurs before the conscious intention, as Benjamin Libet proved with his

well-known experiment.

2.2.1 Readiness Potential (RP) or Bereitschaftpotential

From a physiological point of view, any movement performed or imagined generates visible changes in brain activity, the result of neuronal response to events of different types, such as visual, sensory, auditory or somatosensory stimuli.

These potentials, embedded within the EEG, are called Event-Related Potentials (ERPs) and they are easily extractable through the averaging technique. ERPs are characterized by a sequence of positive and negative deflections, which vary in amplitude, polarity, latency and distribution on the scalp.

The ERPs family contains the category of the "slow potentials," that define the variations of the brain activity related to a psychomotor task: to this type of potentials, belong the Contingent Negative Variation (CNV) and the Readiness Potential (RP), also called Bereitschaftpotential (BP).

The Bereitschaftpotential is a cortical potential which represents the slow cortical activity preceding self-initiated volitional movements.

The first scientists who discovered the BP were Kornhuber and Deeke (1964), who carried out a simple experiment recording EEG and EMG signals while a subject performed a repeated, voluntary flexion of the right index finger at a self-paced rate. Thanks to chronologically reversed averaging technique, they managed to identify three different components in the cortical signals (Figure 2.9), which appear before the EMG onset and represent the preparation for the movement[24]:

- **Bereitschaftpotential (BP)** is a slow cortical negativity detected 2 s or 1.5 s before the voluntary movement and it is bilateral even with unilateral movements;
- **Pre-Motion Positivity (PMP)** is a bilateral cortical positivity that occurs about 90-80 ms before the EMG onset;
- **Motor Potential (MP)** is an unilateral negative potential, that becomes visible about 60-50 ms before the movements. Together with the PMP, it is superimposed to BP and it arises only in the contralateral motor cortex respect to the movement side.

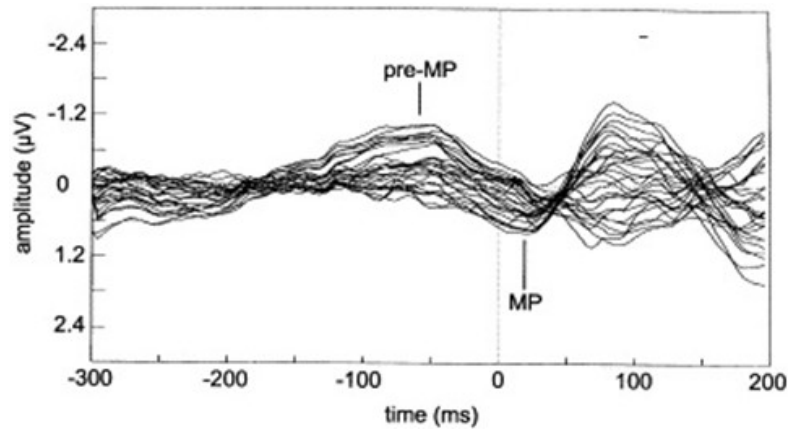


Figure 2.9: Bereitschaftspotential (BP) with the superposition of the Pre-Motor Positivity (PMP) and the Motor Potential (MP):

Shibasaki et al. used a different method while referring to BP, dividing it into two segments: the “early BP” and the “late BP” (Figure 2.10).[24]

- *Early BP* reflects a set of cognitive processes such as attention, preparatory state, movement selection, intention to act which remains unconscious. It is related to subconscious readiness for the following movement, so it is bilaterally symmetrical and arises in the pre-supplementary motor area (pre-SMA).
- *Late BP*, until getting to the BP peak, is influenced by the movement itself such as precision, effort, and complexity, reflecting the conscious will to act. It becomes maximum over the contralateral primary motor cortex for hand movements, and at the midline for foot movements. This asymmetric distribution was identified by Coles as *Lateralized Readiness Potential* (LRP), which derives from the subtraction between the potential recorded at C4 and C3, for both the left-hand movement and the right-hand movement separately.

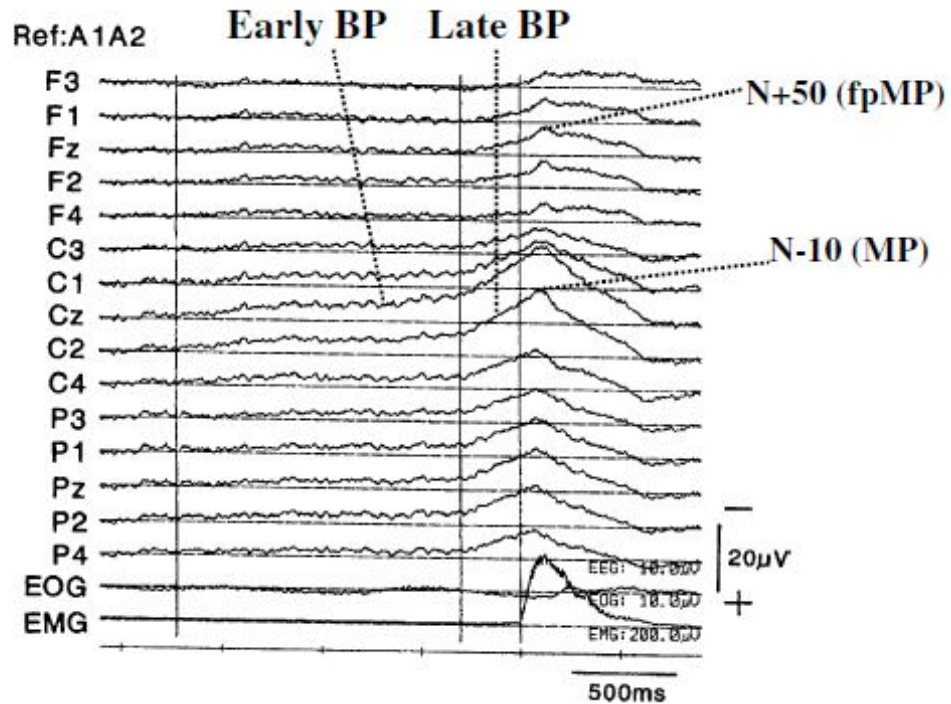


Figure 2.10: Representation of the early and late component of a RP.

As a Movement-Related Cortical Potential (MRCP), the BP is time-locked to an event, connected to the movement, and it is an index of motor preparation. Many factors influence the magnitude and the time course of BP recorded at a self-paced condition, such as preparatory states, level of intention, free movement selection, learning, pace of movement repetition or perceived effort.[24] Another issue that determines the BP waveform and its time course is the effect of discreteness of the movement: Kitamura et al. (1993) compared isolated extension of the middle finger with simultaneous extension of the middle and index fingers, finding a larger amplitude of late BP in the middle finger only movement, despite the simultaneous movement of the two fingers involves a larger number of muscles, underlying the importance of discreteness of the movement. Also the speed of the movement is a crucial element for the amplitude of the BP: the faster is the movement, the later the BP begins. Even the complexity of the movement enhances only the late BP: Benecke et al. found larger late BP before the sequential performance of isotonic elbow flexion and isometric finger flexion than before the single tasks alone, due to the fact that a larger number of muscles were involved in the complex movement than in the simple one.[24]

The Bereitschaftspotential highlights that, before the awareness of the intention to move, there is a subconscious readiness for the movement, represented by the slow increasing cortical excitability elicited by the early BP, while late BP reflects conscious preparation for intended movement.

2.2.2 Lateralized Readiness Potential (LRP)

The Lateralized Readiness Potential (LRP) reflects the particular characteristic of Bereitschaftspotential to present larger amplitudes only on the hemisphere contralateral to the part of the body where the muscle contraction occurs, shortly before the onset of the unilateral motor response.

This lateralization results maximum in correspondence of the motor cortex and the supplementary motor areas: as hypothesized by Kutas and Donchin (1980), the lateralized activation of such areas would indicate that the beginning of lateralization coincides with the moment when the subject decides the side with which he/she performs the movement (for example, right hand or left hand), then the conscious intention of the movement appears (the previous phase, the "early BP", is in fact symmetrical in the two hemispheres, as it indicates the unconscious neuronal preparation to the movement).[25]



Figure 2.11: Topographic distribution of the lateralized current on the scalp when the readiness potential is generated.

The most widely used method for obtaining LRP is the **Double Subtraction Method**, first implemented by De Jong (1988), who introduces the concept of *motor asymmetry*, to indicate the potential difference between two opposite sites of

the scalp due only to the lateralization of the RP.

In fact, the difference between potentials could be due not only to the difference between the RPs but also to other asymmetries between the hemispheres: the double subtraction method allows to obtain the difference between the "pure" RPs, because the difference due to the asymmetries between the hemispheres is independent of the task carried out, then it is canceled, as it is equal whether the activity is carried out with the right side or with the left side of the body.[26, 25] The double subtraction method requires the recording of the RPs resulting from the same task performed with the right side and the left side:

1. The first subtraction consists in the amplitude difference between the RP belonging to the C3 and C4 channels (placed at the primary motor cortex level), both for the task with the right side and for the task with the left side. To each of the two differences, right and left, must be added the contribution related to the inherent asymmetry between the hemispheres, equal in both cases;
2. The second subtraction consists in subtracting the two differences obtained at the previous point, that are the difference between the RP of C3 and C4 resulting from the right task and the difference between the RP of C3 and C4 obtained from the left task (the contribution due to the asymmetry of the two hemispheres is eliminated with this difference).

What is obtained is a parameter, called by De Jong **Correct Motor Asymmetry (CMA)**, which in healthy subjects is a positive value and indicates the extent of lateralization of the RP.

Several studies have shown that such RP lateralization is also generated during motor imagery conditions, with smaller amplitudes of the LRP. Jeannerod (2001) proposed the *Neural Simulation Theory*, which states that motor imagery is a covert action that differs from an overt action only in that the action is not executed, so preparatory brain activity is the same for overt and covert actions.

Rosebaum and Kornblum (1982) developed the so-called **Motor Priming Paradigm**, in which two stimulus occurs before the execution of the task: the first stimulus informs the subject about particular aspects of the movement to be execute after the second stimulus. In the interval between the two stimuli, a rising cortical negativity can be observed in the contralateral side to the effective hand, which indicates that, even if the subject is just imagining the task he has to do after the second stimulus, the motor preparation is specific to the response hand.[25]

2.2.3 Libet's Experiment

In the early '80s, Benjamin Libet and his group carried out a series of experiment aimed to reject the theory of mind-body causation, which implies that motor conscious intention drive motor areas of the brain, that activates muscle in order to execute a movement.

Libet wanted to affirm that conscious experience is a consequence of brain activity, rather than its cause: by studying the relationship between the rise of conscious intention and the BP, he discovered that BP begins about 350 ms before the subject prepares the motor act, therefore before there is conscious awareness of having decided to perform the movement. What Libet argues is that the brain already knows what the selected movement will be much before the subject is aware of it, so there is a delay in the conscious experience of an event.[26]

One of the experiments carried out by Libet consists in asking a subject to fixate a spot rotating every 2560 ms on a screen and to move the right hand whenever the spot was at one of the quadrants, indicating when they felt the “urge to move”, so when the conscious intention arises.[22, 26]

EEG and EMG signals were recorded during the motor task. Libet compared the time when the subject said to feel the “urge to move”, so the conscious intention to move (so-called “W judgement”), with the rising time of the Readiness Potential: the W judgement was 206 ms before the EMG onset, but RP preceded it by several hundred milliseconds. This result suggests that the initiation of action involves an unconscious neural process, which eventually produces the conscious experience of intention. Libet recognized almost three cerebral events that precede the movement (Figure 2.12): the conscious decision to move the limb (W), the unconscious brain event that prepares the motor action (C), the corresponding muscle movement (M).

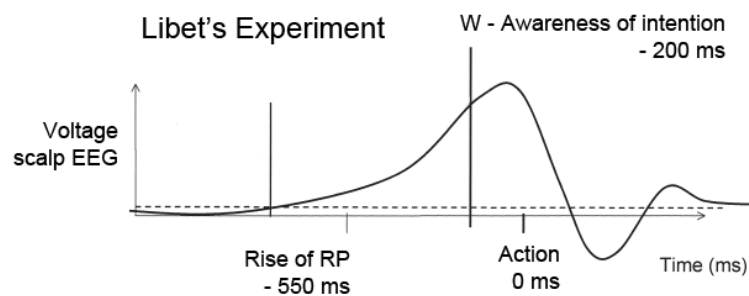


Figure 2.12: Libet's distribution of events that occur at the brain level before a motor task

Taking into reference the muscle movement, the results of the experiment indicate that the moment in which the subject reports to have taken the decision to act (W) occur 200 ms before the action itself, and that the first recorded RP peak is at 550 ms from the EMG onset. It follows that the correct chain of events is RP (-550 ms), W (-200 ms), M (0 ms). In conclusion, RP indicates a preparation of the action that precedes the awareness of the intention to act of at least 300 ms.[22]

Chapter 3

Readiness Potential Recording: Materials and Methods

Readiness potentials are the main characters of this project: the final aim is to obtain clear brain signals after careful pre-processing, create a template of the neural response in different conditions, in order to classify the cerebral state of the subject relying on the obtained waveform.

The first step is the recording of biosignals involved in the study: this experimental phase was performed at *Centro Puzzle* in Turin, recruiting healthy volunteers (control group), both males and females, aged between 18 and 65 years. Potentials were recorded and displayed on screen thanks to *Galileo NT* and its software.

Three different types of biopotentials were needed for the study:

- **Electroencephalography (EEG) signals**, acquired by using an EEG cap with 4, 8 or 32 passive Ag/AgCl electrodes, according to the type of protocol. The EEG datasets were recorded with a sampling frequency of 512 Hz;
- **Electrooculography (EOG) signals**, recorded by placing two adhesive electrodes above and below each eye, in order to increase the effectiveness of the ocular artifacts removal (only in the last protocol);
- **Electromyography (EMG) signals**, acquired by placing adhesive electrodes near the muscles of which the electrical activity is wanted to record. For the last protocol, they are placed on the front and the back of the second phalanx of the index finger, because the required task was the right index lift.

3.1 Tasks and Protocols

Over the years, many protocols have been used, which requires different types of tasks and experimental setups. The datasets on which the pre-processing part of this study (discussed in the following chapter) is applied belong to the last protocol, drafted and used in the *June 2018* recordings.

3.1.1 2012-2015 Protocol

The experimenter starts the clock timer displayed on the computer: starting from 5 seconds, the subject flexes the index finger of the right hand once every 10 seconds for 6 minutes (total 40 epochs). In addition to this standard test, alternative tests were carried out:

- *Using the mouse*: instead of bending the index, the movement is obtained by clicking the mouse button;
- *Using both hands*: in order to remove the stereotyped movement effect, the subject in question uses both hands and the experimenter indicates which;
- *Short trials*: The experiment is performed as the standard one, but with a smaller duration of trials (5 seconds). The aim is to validate the hypothesis of lack of free will: the subject becomes aware of the action to be performed after the preparation of the brain for such action (Libet experiment).
- *Bimanual*: The experiment is performed with both hands at the same time. This type of task arises from the need to investigate the cognitive conditions of patients with *anosognosia for hemiplegia*, a transient condition that, in some cases, can affect subjects where stroke has involved the right hemisphere of the brain, damaging the motor area. In such subjects, there is a paralysis of the left side of the body, but the patient himself is not aware of it, he openly claims to have no problem and to be able to move correctly both the arm and the leg paralyzed.

To pick up the EMG signal from such subjects, which are paralyzed only for the left side of the body, you need to ask to move both hands (hence, the name of the task "Bimanual"): the not impaired hand performs the task and allows the withdrawal of the signal, while for the immobilized hand the patient imagines the movement, which he actually believes to accomplish.

The patients in which this pathology is found are totally right-sided injured: if the stroke affects the left hemisphere, the center of the language is also compromised, so they could not express their degree of awareness about paralysis.

3.1.2 2015-2018 Protocol

In the experiment, it is required to make a simple movement, observing a clock projected on a screen: starting from the second 5, the movement is repeated every 10 seconds, for 6 minutes and 40 seconds, for 40 epochs in total. Among the movements required, there are: the flexion of the index finger, the voluntary movement of the foot or leg, the coordinated movement of the hand and leg and the patellar reflex of the knee.

Some tasks are performed with the subject blindfolded: in this case, the operator observes the watch and gives the subject an indication of when to make the movement, to avoid influencing the external environment on the subject.

3.1.3 2018 Protocol

The subject performs finger movement, recording the EMG signal (Figure 3.1). Neurologically healthy volunteers perform three tasks in each test session:

- *Voluntary task*, in which the subject must move the index finger. The movement must take place in a time window of 10-13 seconds, starting by a beep. This experiment aims to enclose the movement in a fixed time frame, but gives the subject the opportunity to make a voluntary choice, which then varies from person to person and trial to trial.
- *Semi-voluntary task*, in which the subject repeats the same movement as the previous task, but in this case he/she moves the index finger as soon as he/she hears the beep.
- *Involuntary task*, requires the patellar reflex to be stimulated at the tendon by means of a gavel. For this task, the acoustic signal is only perceived by the experimenter wearing headphones, so that the subject cannot predict the exact moment when he will receive the stimulus.

Each experimental session consists of 40 repetitions for each task and the acoustic signal is randomized to avoid adaptation by the subject.

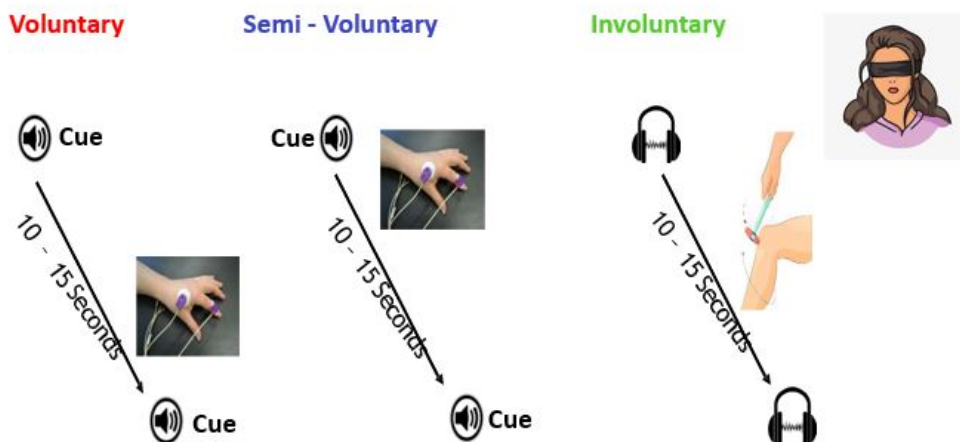


Figure 3.1: 2018 Protocol for EEG, EOG and EMG recordings (voluntary, semi-voluntary and involuntary task).

3.1.4 Datasets: classification

Data related to the three protocols and the different tasks have been classified and named based on the subject information, the type and mode of acquisition of biological signals and the specifications of the instrumentation used.

In this protocol, a *Labjack* is used, which is a USB based measurement and automation device, that provides digital inputs/outputs, in this case the trigger for the movement, while connected with a Data Acquisition System (DAQ).

In the adopted classification, both the EMG signal and the Labjack signal were evaluated through a scale ranging from 0 to 3, where 0 indicates that the signal has a poor quality, while 3 indicates a good quality signal. The EMG signal quality considerations are based on the variability of the signal itself and the amount of noise.

Datasets have a name composed of a string of 45 characters. More in detail, there are:

- **8 characters** bearing the anonymized name of the subject, so sequentially the first letter of the name, the first letter of the surname, the last digit of the recording year, the last two digits of the year of birth, the month of registration and the character 0/1 if the subject is male/female (in case of homonymy, the last character is placed equal to 2);
- **5 characters** for the EEG electrode mounting: 32C18 is the acronym for the 32-electrode mounting ("32 Channels 2018"), while OBE12 is the one with bridge electrodes ("Bridge Electrodes 2012");

- **4 characters** indicating the protocol used for the control group: A18C for the 2018 protocol ("After 2018 Controls"), B18C for the 2015-2018 protocol ("Before 2018 Controls") and VOPC refers to the data of the 2012-2015 protocol ("Very Old Protocol Controls");
- **3 characters** to describe the condition of the subject: the acronym FOL refers to blindfolded subjects, while UNF to non-blindfolded;
- **5 characters** to identify the type of task performed: voluntary, semi-voluntary or involuntary, indicated respectively by VOL18, SEM18 or INV18;
- **4 characters** for the task: RFOF for right forefinger, LFOF for left forefinger, BFOF for bimanual forefinger, RMOU when clicking the mouse with the right hand, RLEG for right leg, LLEG for left leg, RFOO for right foot, LFOO for left foot, RHLE for right hand and leg, LHLE for left hand and leg;
- **4 characters** to indicate the channel used for EMG: EMG1 for channel 1, EMG2 for channel 2, EMGX for channel without any number;
- **4 characters** to discriminate signal quality for EMG and Labjack, therefore: E + 0/1/2/3 for EMG and L+ 0/1/2/3 for the Labjack (in protocols prior to the 2018 protocol, the last two characters correspond to L0, as LabJack is not present).

3.2 Experimental setup

In this section, the materials and the preparation stage are described, according to the last protocol, drafted in 2018. Before starting with the recording phase, it's important to carefully fix the instrumentation in a suitable way, in order to acquire a legible signal trace (Figure 3.2).

Such instrumentation is composed by:

- **Data Acquisition device:** Galileo Suite, EB Neuro with Brain Explorer (BE) amplifiers;
- **Galileo Software** for processing and display the EEG traces;
- **Stimulation system:** Labjack and OpenSesame software for the acoustic signal;
- **Synchronization system:** Labjack and photocoupler circuit;
- **Recording tools:** EEG cap, adhesive electrodes (4 for EOG signal and 2 for EMG signal), the ground electrode for EMG (placed on the wrist for voluntary

and semi-voluntary tasks or on the ankle involuntary task), 2 earlobes reference electrodes for EEG;

- **Additional accessories:** TEN20 (conductive paste), NUPREP (abrasive paste), conductive EEG gel, a syringe with a blunt needle.



Figure 3.2: Experimental setup in *Centro Puzzle*, Turin

During the recordings, the subject is sitting on a raised chair to avoid the feet from touching the floor, especially in the involuntary task, that is the patellar reflex.

Two computers are needed: the first one, in which the *OpenSesame* software is installed, is useful for starting the task and emitting the acoustic signal, the second one, in which there is *Galileo* software connected to the EEG cap, is used to visualize, process, but also export subsequently, the acquired signals.

The subject is then seated behind the first computer, while the second one is placed turning left from the position in which he is sitting, so as not to be influenced in any way during the experiment.

Regarding the positioning of the electrodes, firstly EMG and EOG sensors and then the earlobes and the wrist (or the ankle for the involuntary task) electrodes are mounted, using TAN20 paste. Subsequently, the EEG cap is set on the head, trying to position the Cz electrode in the middle between *nasion* and *inion* and

between the two earlobes reference electrodes. After placing the cap, the skin is cleaned, using the NUPREP abrasive paste, in order to remove sebum and dead scalp cells. Then, the inside of the cap is filled with the conductive EEG gel, through a syringe with a blunt needle.

The conductive EEG gel is useful for two reasons:

- **to improve signal conduction**, lowering the electrode impedance, in order to obtain a good electrode-skin coupling. Therefore, before acquiring the EEG signal, the experimenter has to check that the electrodes' impedance does not exceed a certain threshold value, equal to 10 k;
- **to improve adhesion** with the skin, avoiding any problem of detachment caused by movement.

3.3 Software for signal processing

After acquiring the biosignals and making them compatible with the Matlab environment, they must undergo careful processing, in order to improve their quality and eliminate any disturbing elements, which could affect the subsequent classification.

To elaborate these potentials, the EEGLAB toolbox has been used, in particular the MRCPLAB plugin, created specifically for the purposes of this project, of which the functionalities will be briefly described in the following sections.

3.3.1 EEGLAB

EEGLAB is an interactive Matlab toolbox, distributed by Swartz Center for Computation Neuroscience (SCCN), for processing continuous and event-related EEG, MEG and other electrophysiological data.

It allows independent component analysis (ICA), time/frequency analysis, artifact rejection, event-related statistics, and several useful modes of visualization of the averaged and single-trial data.

Providing an interactive graphic user interface (GUI), EEGLAB offers a wealth of methods for visualizing and modeling event-related brain dynamics, both at the level of individual EEGLAB 'datasets' and/or across a collection of datasets brought together in an EEGLAB 'studysset.'

Furthermore, EEGLAB offers an extensible, open-source platform through which anyone can share new methods with the world research community by publishing EEGLAB 'plug-in' functions that appear automatically in the EEGLAB menu of users who download them: MRCPLAB, implemented for analyzing movement-related cortical potentials (MRCPs), is a valid example (Figure 3.3).

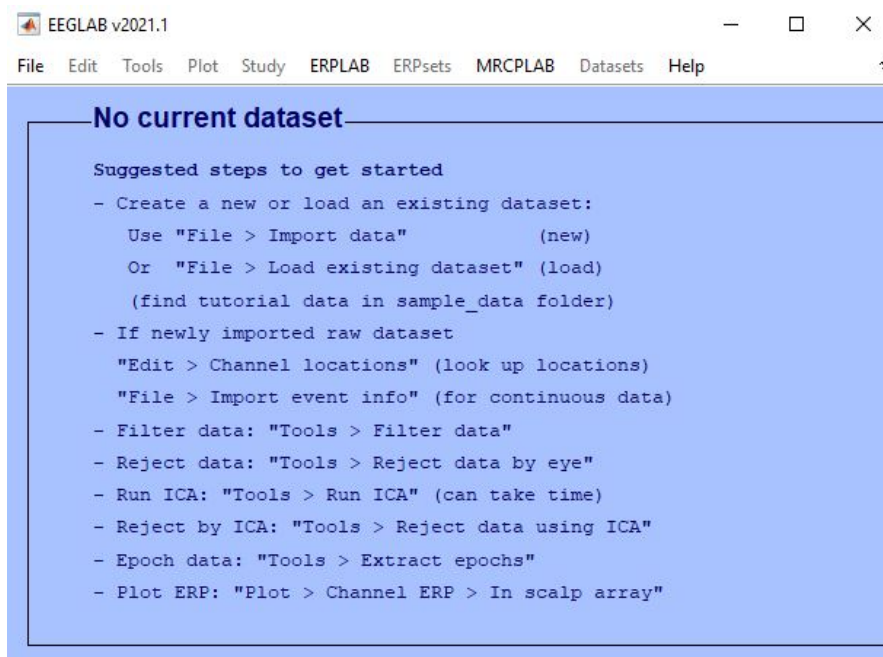


Figure 3.3: EEGLAB Graphical User Interface: for this project, the menu MRCPLAB and its sub-menu are used.

3.3.2 MRCPLAB

In order to process the EEG data acquired by the software *Galileo NT*, a plug-in has been developed for EEGLAB, called MRCPLAB, which manages to integrate all the algorithms implemented with EEGLAB and also adds very useful functions to analyse the MRCP signal automatically.

In particular, from MRCPLAB, appears a drop-down menu in which:

- **Import/Save Data** is used to import a dataset, saving it in the format *.set* and making it compatible with EEGLAB (Figure 3.4). If the option *Import from ASCII file and filter* is selected, EEG, EOG and EMG signals are imported and temporally filtered, after the EMG onset detection.

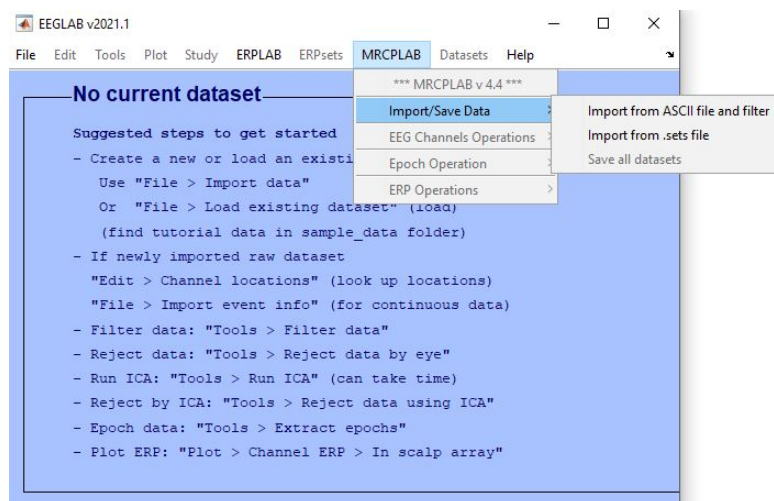


Figure 3.4: MRCPLAB and "Import/Save Data" Menu.

More in details, when choosing to process a dataset in the format *.asc*, the plug-in opens an interactive window, which asks the user to enter information, including:

- The sampling frequency;
- The epoch duration, in seconds, in which the signal is divided, which is equal to 10 seconds for the datasets acquired before June 2018 or it's 0 if the input signal is provided by the Labjack, used for datasets acquired after June 2018;
- The epoch definition, in milliseconds, which is already set;
- The channel on which the EMG signal is detected, which may be EMG1 or EMG2. It was also used another channel, called "Pulsante" for the acquisition of the EMG signal, that must be entered in this box if the dataset name reports the EMGX as EMG channel;
- The name of the cue channel, which is the Labjack for experiments conducted on healthy volunteers;
- In the end, the user can choose whether to obtain a graph with the EMG trace or the EMG with the cue channel signal.

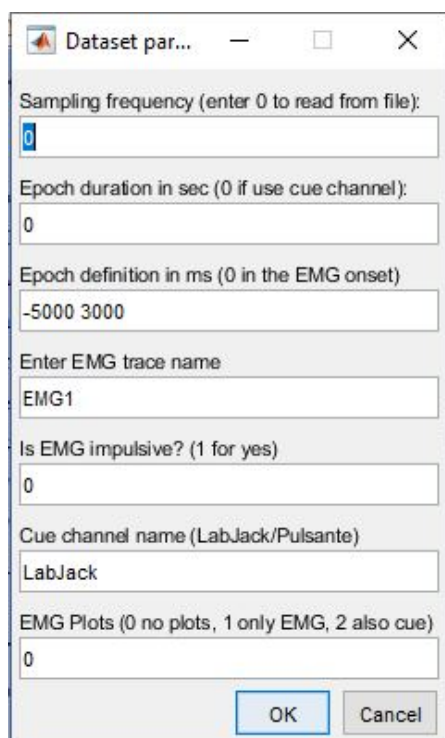


Figure 3.5: Dataset parameters settings while importing datasets.

If the dataset is already saved in local memory as “.set” file because it was already imported and filtered, the option *Import from .sets file* can be selected. At the end, three different datasets are created, which contain 1) EEG signal filtered, 2) EEG, EOG and EMG signals filtered and 3) EOG with EMG signals filtered.

- **EEG Channel Operations** allows to carry out actions on the EEG channels (Figure 3.6):
 - *Channel data scroll*, for visual analysis of EEG signals related to all channels;
 - *Seek noisy channels*, for detecting particularly noisy channels relying on channel statistics;
 - *Select or reject data* for maintaining or deleting portions of data, such as temporal ranges, epochs or entire channels;
 - *Artifact correction*, for correcting and eliminating distortions and signal disturbances that do not contain significant information about neuronal behaviour, using the Independent Component Analysis (ICA);

- *Interpolate electrodes*, for substituting channels removed in the previous steps with the interpolation of the surrounding channels, useful to allow the comparison of the scalp distributions across subjects. Two interpolation methods have been implemented: the nearest-neighbor interpolation, replacing one site with the average of the neighboring sites, and the spherical spline interpolation that takes into account all of the electrode sites.;
- *Spatial filtering*, for computing clearer spatial maps, scalp potentials densities or scalp current densities, highlighting the source of the neural event. For each channel, a virtual channel is computed, in order to filter out the spatial low-frequency components.

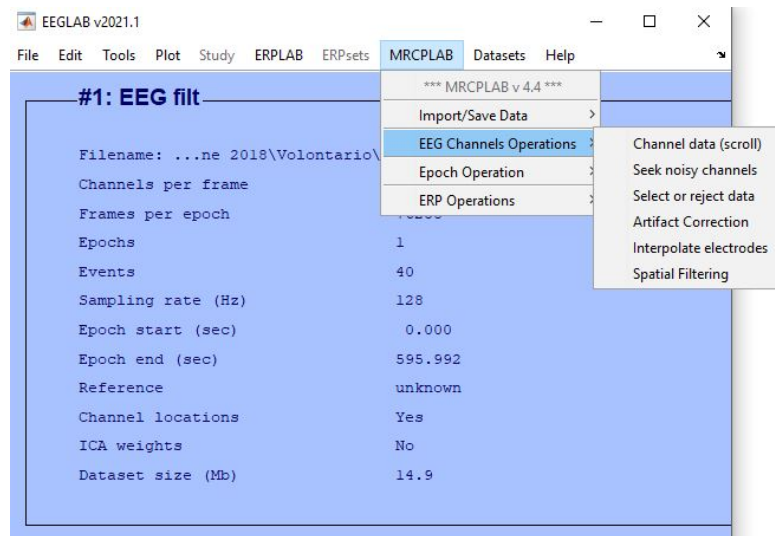


Figure 3.6: MRCPLAB and "EEG Channel Operations" Menu.

- **Epoch Operations** contains:
 - *Epoch calculation*, for computing the epoching, starting from the EMG onset that is pointing to zero and considering 5000 ms before and 3000 ms after the onset. It also allows the baseline removal, which is a low-frequency drift coming from the background fluctuations that appears in the first part of the epoch, when the subject has not received the stimulus yet.
 - *Jitter Compensation*, for aligning the epochs affected by sample delays, in order to improve the quality of the signal when averaging the epochs.
- **ERP Operations**, through the command *ERP Viewer*, shows the ERP signal, obtained by averaging all the epochs for every channel.

Chapter 4

Jitter Compensation

4.1 Trial-to-trial latency variability

Event-related brain potentials (ERPs) are frequently employed in Cognitive Neuroscience, because they provide information about mental processing due to an external stimulus with a high temporal resolution.

However, their usefulness is limited by the need to average over a large number of trials: aiming to obtain a Readiness Potential (RP), this project had to deal with the problem of the *trial-to-trial latency variability*, that can affect EEG epochs and may blur the average ERP waveforms, attenuating their amplitude and hiding relevant physiological meaning about the effects of a specific condition.

ERPs are obtained by averaging many epochs of EEG from single trials, assuming that the stimulus related signal embedded in the EEG occurs identically from trial to trial, and that the random background noise statistically averages to zero across trials.

Averaging is very sensitive to latency jitter, which is a timing misalignment of the epochs used to compute the RP, due to small changes in the brain times across all the trials and movements' onsets timing detection.

Many studies have revealed that ERPs components strongly vary in latency across all trials, resulting in a smearing effect which cause the average ERP's amplitude attenuation.

Such issue can induce unwanted effects in two different situations:

1. When considering different conditions characterized by *different ERP's amplitudes* but *same trial-to-trial latency variability*, it's possible not to distinguish the difference of amplitudes between conditions: being the amplitudes reduced, the background noise could be of the same order of magnitude as the effective signal, preventing the correct detection and identification of the potential and

affecting its statistical parameters.

2. When considering different conditions characterized by *same ERP's amplitudes* but *different trial-to-trial latency variability*, different amplitude attenuation may occur, mimicking an amplitude difference between conditions that in reality doesn't exist. Such differences can be erroneously attributed to different strength of activity by the underlying neural system.

In both cases, as shown in Figure 4.1, this latency variability and the resulting distortion of the single trial ERP in the averaged waveform can lead to erroneous conclusions: obscured amplitude difference in the first case, when different conditions requires it, and enhanced amplitude difference in the second case, when there is no difference at all.[27]

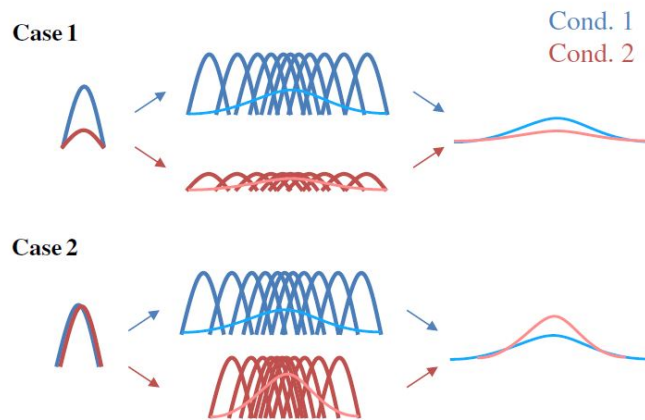


Figure 4.1: Comparing different conditions, the smearing effect of trial-to-trial latency variability induces errors in the resulting averaged waveform.[27]

Case 1: Different amplitudes and same latency variability induce indistinguishable difference of amplitude in the final ERP.

Case 2: Same amplitudes and different latency variability mimic an erroneous amplitude difference between conditions.

The challenge for this thesis work is the implementation of an automatic algorithm, Residue Iteration Decomposition (RIDE) Method (Ouyang et al., 2015), which allows to decompose ERPs into many component clusters with different latency variability and to re-synchronize the separated components, in order to obtain a reconstructed ERP as closer as possible to the single trial waveform.[28]

4.2 Previous attempts

Many studies have been conducted on the problem of jitter compensation in ERP data, but it has not come to a single solution. An event-related potential waveform, as such, shows several components, which reflect what happens at the neuronal level corresponding to the stimulus onset and to the motor response, which is generally delayed.

As shown in Figure 4.2, the original assumption that the single trial waveform consists in a single stimulus-locked component turned out to be unrealistic: it may comprise several components with different latency across trials, that averaging may blur or attenuate.

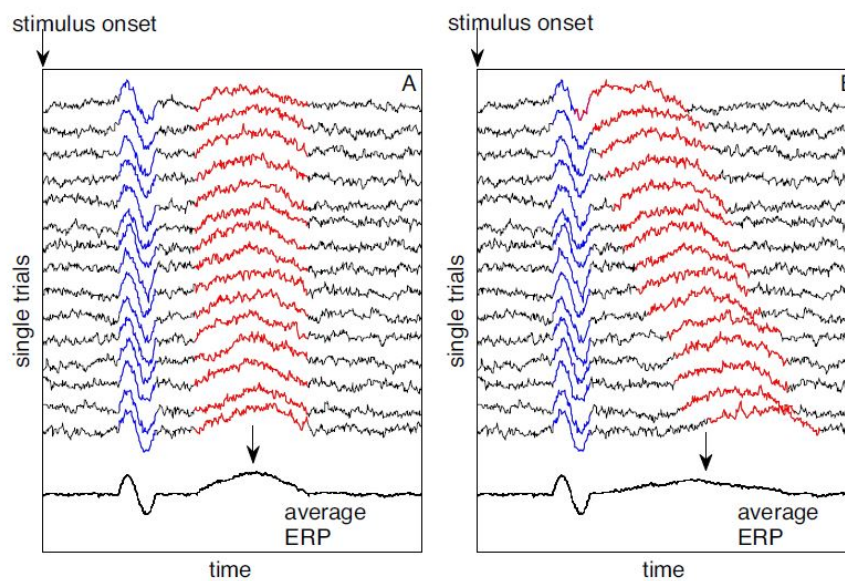


Figure 4.2: ERPs obtained by averaging single trials with components temporally locked to the stimulus onset (A) or not temporally locked to the stimulus onset (B). [28]

Several solutions have been investigated over the years, in order to reduce the negative effect of latency jitter in averaged ERPs:

- i. The traditional method for jitter compensation consists in response-locked averaging, relying on the assumption that the late ERP components will come out more clearly when synchronized to the response.

It has some limitations:

- a) it can compromise the stimulus-locked components;
- b) several tasks do not require any response;

- c) some ERP's components can be neither stimulus-locked nor response-locked, so can be blurred by the response-locked averaging.
- ii. A reinterpretation of the previous method consists in considering the event-related potential solely as a set of marker-locked components, where markers can be external events such as stimulus onset, response times or other cues. The main limitation of this method lies in not taking into account the existence of components that are not related to the considered markers or show relations with two or more of them.
- iii. Jung's (2001) approach involves Independent Component Analysis (ICA) in order to separate the ERP waveform into different components with variable latency: it results in a large cluster of independent components difficult to classify, because locked to not distinguishable markers.[27]

In all these attempts in solving the latency jitter issue, an underlying problem can be recognized: whether stimulus-locked, response-locked or marker-locked averaging is, the resulting ERP ends up increasing the resolution of a certain component by sacrificing the resolution of other components, which can be related to different markers or not locked at all, as clearly shown in Figure 4.3.

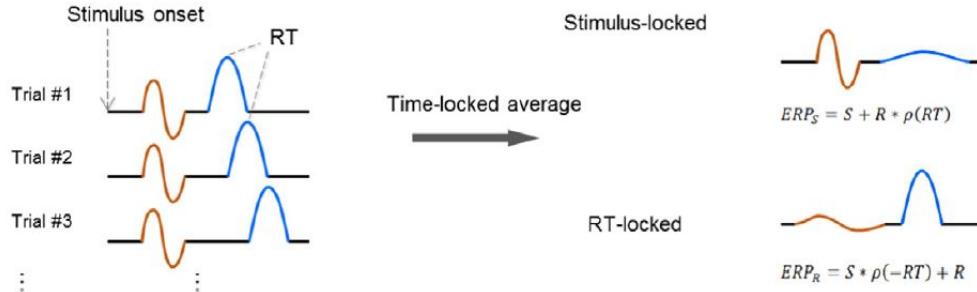


Figure 4.3: Stimulus-locked and response-locked averaged ERPs – each method smears the other component.

Furthermore, if two or more components are detected, common ERP averaging is not able to deal with the higher level of complexity of the analysis, since the amplitude effects will be embedded into several parts of the signal. Also in this project, an attempt to counteract the negative effects of trial-to-trial latency variability has been made: the approach used previously, already present within the MRCPLAB plug-in, is the Woody's method, based on the cross-correlation between the single epochs.

4.2.1 Woody's Method

Woody's Method iteratively calculates the cross-correlation between each trial signal and a template, obtained by averaging the trial signals whose the time delay is shifted by the delay estimated in the previous iteration.

It is the simplest method for implementing jitter compensation, mainly because it involves the Pearson's correlation, which is easy and quick to calculate but it captures only linear relationship, presuming that the brain underlies linear systems.[29]

In this section, Woody's Method is briefly described, in order to better understand the system already implemented in the plug-in and analyze the reasons that have encouraged the introduction of a more performing method, the Residue Iteration Decomposition (RIDE) Method.

When computing cross-correlation between two generic epochs, what is considered is the linear index corresponding to the maximum of the cross-correlation function. Step by step, the Woody's Method requires:

1. The creation of a correlation matrix among all epochs, using all the possible combinations between the generic epoch i and the generic epoch j . For every epoch, the median value of correlation is considered and the epoch with the highest median value is selected.
2. Among all the remaining epochs, the most correlated epoch with the previous one is considered.
3. The time delay between the two epochs chosen at the points 1. and 2. is evaluated and such epochs are realigned by shifting the second one as many samples as the estimated delay (Figure 4.4). At this point, after the time shifting, the cross-correlation between the two epochs should have the maximum in zero.
4. The average between the two epochs is calculated, thus obtaining the first template of the RP.
5. The steps are reiterated from point 2., recomputing the cross-correlation function between the RP template and all the remaining epochs. Iterations end when the correlation between the template and all the remaining epochs becomes too small, less than a certain threshold, set by the user.
6. At the end of the iterations, the definitive RP is calculated by averaging all the epochs realigned and not discarded.[29]

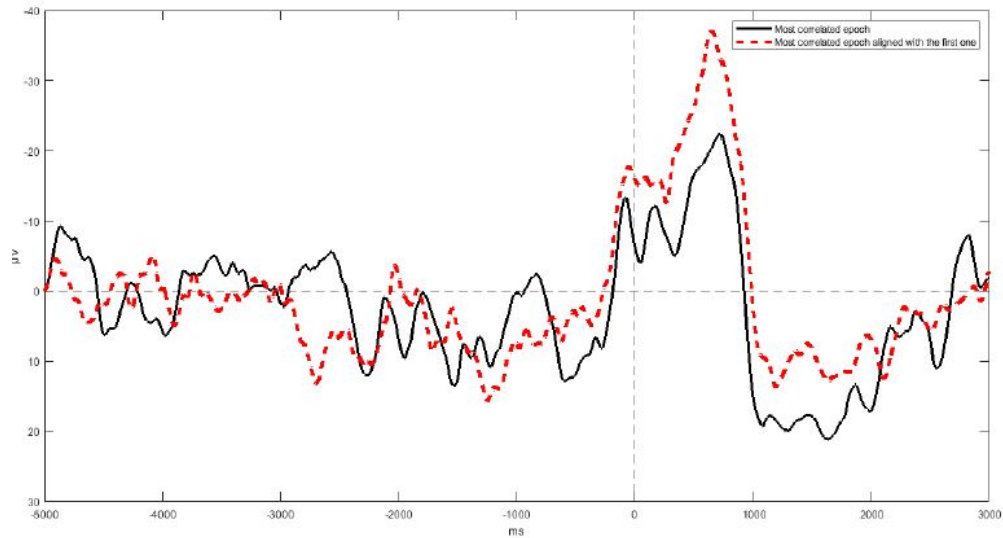


Figure 4.4: The red dashed signal, corresponding to the most correlated epoch with the first one, was aligned with the signal of the most correlated epoch.

Some adjustments have been made to the standard Woody’s Method, to address some problems related to noise and artifacts embedded in the EEG signal. A first problem with this method is that the epoch, which most correlates with all the others and had the highest correlation median value at point 1., does not contain the signal, but only one large artifact. In this case, the reason why it correlates very well with the others may be because of some common artifacts with all the other epochs. For this reason, it is more appropriate to choose as the initial template, the RP obtained by averaging all the epochs, although they have not yet been realigned.

A second issue is that the RP may be immersed in noise, in the case of recordings acquired on patients, so it may help to use as an initial template a signal with the typical waveform of the RP, not obtained from the data but artificially realized by the user.

Compensating the jitter by using the Woody’s algorithm, clear and distinguishable RPs are obtained in most of the datasets examined, both for the voluntary movement task and the semi-voluntary movement task.

Despite this, some limitations came to light, which this thesis work tries to overcome:

- **Dependency on Fcz Channel Latency**

The latency jitter compensation is not computed individually for each channel, but the shift applied to every epoch in order to align it to the one which mostly correlates is calculated for the epochs of the channel Fcz, which is

taken as a reference, and applied in the same way to all the corresponding epochs of the other channels.

This implies that the evolution over time of the event-related potential, which is not distributed in all areas of the cortex simultaneously, do not come out: different channels may show different delays as they are placed at various distances from the point where the potential occurs, reaching the electrodes at different times.

- **Single Stimulus-Locked Component**

Woody’s method relies on the delay compensation between correlated epochs, whose jitter is computed starting from the movement peak.

As already highlighted for other methods, in the study of ERPs, it’s limiting to consider a single component related to only one event-marker, as there may be some ERP’s components which arise independently from the stimulus onset or underlie a mixture of neural responses coming from different events or from no event at all.

The risk is that the components that are not taken into account are attenuated when applying the averaging technique, very sensitive to latency jitter.

4.3 Residue Iteration Decomposition (RIDE)

The *Residue Iteration Decomposition Method* has been developed by Ouyang, Sommer and Zhou for dealing with the limitations of conventional approaches for ERP jitter compensation, starting from the assumption that such potential hides different components, with different single trial latencies.

RIDE combines the information of available time markers, such as the stimulus onset or the response time, and estimates latencies to extract both marker-locked and non-marker-locked component clusters: separating different components and re-synchronize each component to its respective latency, it can avoid the smearing effect of trial-to-trial variability in averaged ERP, that results into blurred waveforms with attenuate amplitudes.

In general, RIDE separates the ERP into three component clusters: the stimulus-locked component **cluster S**, the response-locked component **cluster R** and the central, ‘neither-nor’ component **cluster C**, which is neither relative to the stimulus nor the response, but has significant latency jitter that can be detected by template matching. The separation paradigm can be extended to more components, such as two C components (if the pattern of ERP allows, for example, two clear humps in the late time window), or only S and R, or only S and C in the data without response time (from experiment without RT recorded).

For better understanding the idea of separated components, Figure 4.5 shows four EEG epochs with three component clusters in each single trial: the blue component is locked to the stimulus, whereas the red and the green components are respectively the central component and the response-locked component, which vary their latencies relative to the stimulus from trial to trial. The conventional approach for obtaining the ERP (on the left) blurs the representation of single trial ERPs and decreases the amplitudes; synchronizing each component cluster to its latency across single trials (on the right) helps to obtain an averaged ERPs close to the single trial waveform.

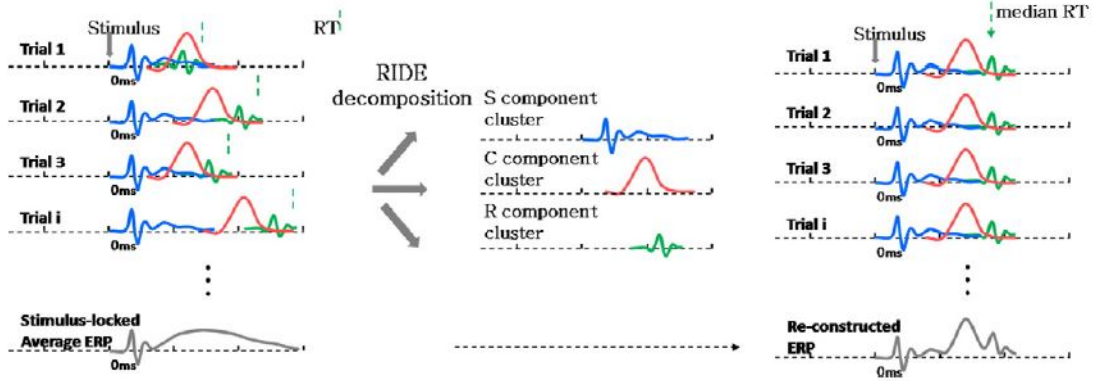


Figure 4.5: Conventional average ERP (left) from single trials with latency jitter, decomposition by RIDE (middle) and reconstructed ERP after correcting for latency variability (right). [27]

4.3.1 ERP model

RIDE relies on the assumption that ERPs embeds different components with variable delays, with random noise in addition:

$$EEG_i(t) = C_1(t - \tau_{1i}) + C_2(t - \tau_{2i}) + \dots + C_n(t - \tau_{ni}) + \xi_i(t) \quad (4.1)$$

where:

- $EEG_i(t)$ is i th single trial of EEG data;
- $C_n(t)$ is the waveform of the n th component;
- τ_{ni} is the latency of the n th component for the i th trial, which varies independently across single trials;
- t is the time coordinate from the stimulus onset, which is set at time zero;

- ξ_i is the noise for the i th trial.

In Equation (4.1), each component is assumed to have constant amplitude across trials, therefore the $ERP(t)$ is the convolution of the components amplitude with the distribution of their latencies across single trials $\rho(\tau_n)$, meaning convolution as a weighted moving average. Noise is omitted assuming a large number of trials, so it statistically averages to zero.

$$ERP(t) = C_1(t) * \rho(\tau_1) + C_2(t) * \rho(\tau_2) + \dots + C_n(t) * \rho(\tau_n) \quad (4.2)$$

In order to avoid the smearing effect of convolution, which blurs the representation of components in the averaged ERP because of the trial-to-trial latency variability, the distribution of latencies $\rho(\tau_n)$ for each component is replaced with the most probable latency across single trials, obtain the most probable ERP.

$$ERP_p(t) = C_1(t) * \delta(t - \tau_{1p}) + C_2(t) * \delta(t - \tau_{2p}) + \dots + C_n(t) * \delta(t - \tau_{np}) \quad (4.3)$$

Equation (4.3) can be simplified as follows, assuming that $C_n(t)$ waveform is the single trial located at the most probable latency:

$$ERP_p(t) = C_1(t) + C_2(t) + \dots + C_n(t) \quad (4.4)$$

As shown in Equation (4.4), the goal of the method is to obtain the time courses of each component $C_i(t)$, which may have explicit or not time markers.

4.3.2 Algorithms and Methods

The RIDE method is implemented as an algorithm of *iterative subtraction*, which separates different clusters of ERP's components according to their time-locking to stimulus onset, response times or estimated latencies, reconstructing ERPs by re-aligning the component clusters to their most probable trial latencies.

The decomposition algorithm consists of four steps, in which there is the succession of a Decomposition Module as an *inner iteration* loop and a Latency Estimation Module as an *outer iteration* loop.

(1) ***Initial estimation of the C component latency in single trials***

While the initial latency of the stimulus-locked and response-locked components is supposed to be known, the latency of the component C is unknown, due to the undefined origin of the component itself.

(2) ***Decomposition Module***

Once obtained the latency of S, C, and R components, this inner iteration module separates the ERP into three component clusters: iteratively, two of the

components are subtracted from the ERP in order to keep the remaining one and aligning the residuals of all trials to the latency of the specific component.

(3) ***Latency Estimation Module***

As opposed to S and R components' latencies, which are fixed and already given to the algorithm, the C component latency has to be computed for each outer iteration, in order to provide an increasingly accurate latency value to the Decomposition Module for inner iterations.

(4) ***Iteration of (2) and (3) until convergence***

In the following paragraph, the different modules are described, which group several detailed algorithms, inserted in the MRCPLAB plug-in.

Initial Latency Estimation Module

The C component has no overt latency information related to external markers, such as stimulus onset or response time.

The initial estimation of L_C (C component latency) can be derived in several ways, but the most common is Woody's Method. In this case, the latency estimation with the Woody's Method is not solely applied to the Fcz channel, but it is extended to the entire electrode set: the cross-correlation between the template and the remaining trials is calculated for each electrode and then averaged across all electrodes. This approach helps to emphasize the contribution of dominant electrodes and weaken the contribution of irrelevant sites. The maximum of the averaged cross-correlation function for each trial is taken as the single trial's latency L_C .

Decomposition Module

It aims to separate S, C and R components, starting from the already known latencies L_S , L_C and L_R .

Initially, $S(t)$, $C(t)$ and $R(t)$ are set to zero: the single components are estimated one by one, removing the other two components and synchronizing the residual trial to the latency of the considered component, obtaining the median waveform for all time points.

For easily understanding, Figure 4.6 shows the steps of Decomposition Module, considering only two components for each trial, but the same reasoning can be applied in case of three or more components.

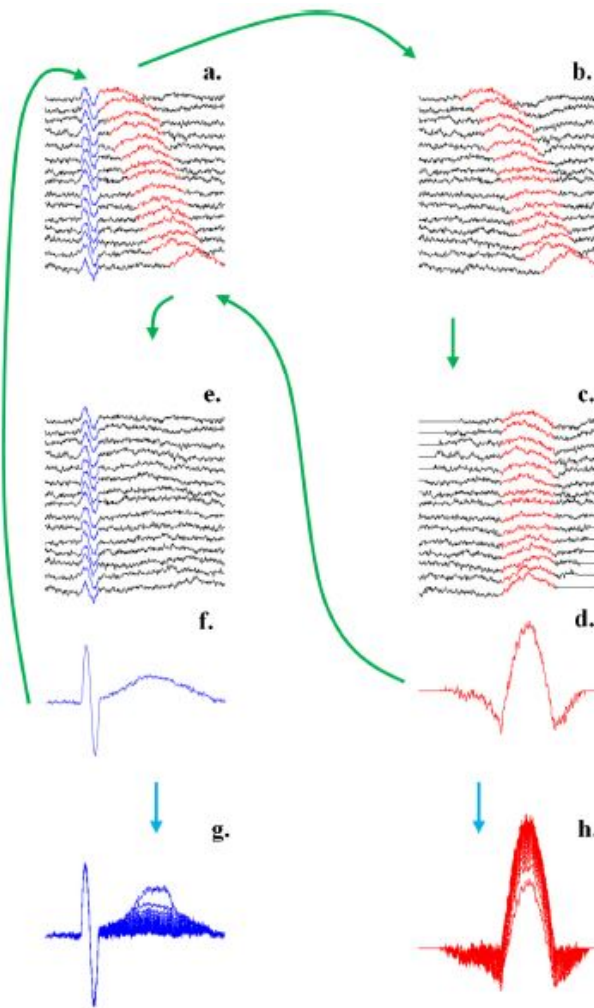


Figure 4.6: Steps for Decomposition Module using two artificial sinusoidal components for a single electrode. [28]

- a. Different trials are plotted, highlighting the superposition of a stimulus-locked component (blue) and a response-locked component (red).
- b. The S waveform is subtracted from all single trials (S is initially stimulus-locked ERP).
- c. The R component is aligned across trials according to the R latency.
- d. The R median waveform for all the time points is obtained from the aligned trials.
- e. The R median waveform is subtracted from all the original single trials (a.).

- f. The S median waveform for all the time points is obtained from the single trials without R component. The steps from b. to f. are repeated, subtracting the S waveform obtain at f. from all trials at point b., until convergence, defined as a small difference ($< 10^{-3}$) between two successive iteration with respect to the two initial iterations.
- g, h. The resulting waveform for S component and R component, obtained at step f. and b., are shown: at each iteration, the component waveforms become closer to the original signal in single trials.

Latency Estimation Module

In order to improve the accuracy of the C component latency, it is again estimated after the separation of components and then used back for the Decomposition Module.

For this step, the template matching technique is used: S and R components are removed from each original single trial and the cross-correlation between the single trial residue (original C component) and the C component obtained in the last decomposition iteration (template) is computed.

Also in this case, the cross-correlation function is averaged across all the electrodes and its peak is taken as the new L_C for the next decomposition. Also such outer iterations for the latency estimation are repeated until convergence of the C component latency.

Additional items: Baseline Correction, Low-Pass Filter and Amplitude Estimation

- After every decomposition module, a baseline correction is implemented for each component, in order to adjust the baseline of component S to the same baseline value of conventional average ERPs in the early time window $[0, t_e]$ and to set the components C and R to zero baseline values in $[0, t_e]$. This operation relies on the assumption that waveforms in the early period should be in line with the original ERP for the stimulus-locked component cluster S and should be zero for the later component clusters (C, R), since they are not yet active. t_e is set to 200 ms by default.
- When computing the C component latency estimation, it's necessary to apply a low-pass filter, in order to avoid distortion in the cross-correlation function, due to intrinsic high-frequency oscillatory noise of EEG data, that can be absorbed to the C component clusters and affect the iteration result. A 3-5 Hz low-pass filter has been found to be optimal in general cases.

- The amplitude of RIDE components for each single trial and each single channel is estimated by covariance between the specific component obtained by RIDE decomposition (template) and the original single trial after removal of other RIDE component. The covariance is only calculated within the time window specified for each RIDE component.

Outcome Module

As described in Section 4.3.1 and stated by the Equation (4.3) and (4.4), the reconstructed ERP is obtained by the **summation of each RIDE component**, synchronized to its probable latency. In this case, the robust median value is used as an approximation of the most probable latency.

As a result, the ERP can be reconstructed in a de-blurred way, as Figure 4.2 shows: it displays enhanced amplitudes and richer waveform patterns with respect to the conventional averaged ERP.

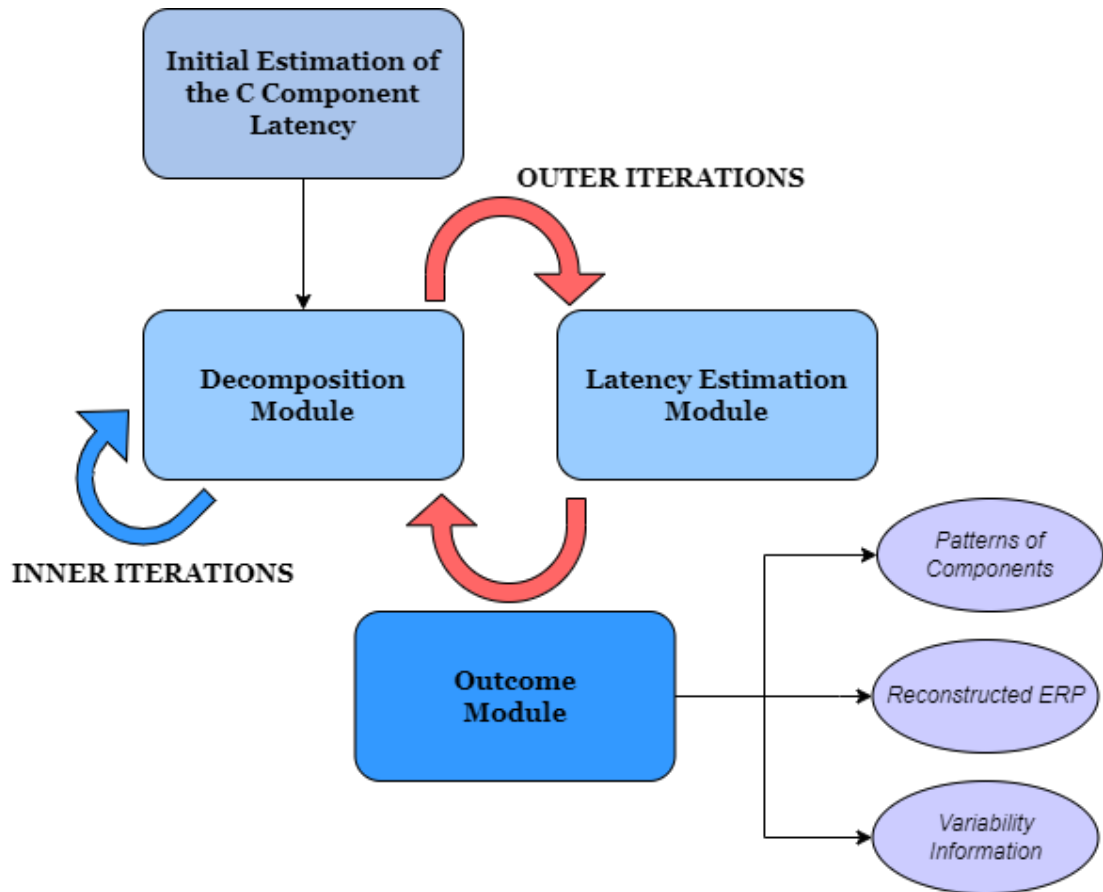


Figure 4.7: RIDE algorithm workflow.

4.3.3 Input Parameters and Output Variables

Before running RIDE algorithm, data should be prepared in the Matlab workspace, in order to be processed in the correct way.

RIDE toolbox requires that the single trial data are segmented and prepared as a 3D matrix (*time x number of electrodes x trials*).

RIDE toolbox need to fed the main function with some input information about signal's timing and components.

All the input parameters are saved in the structured variable *cfg*, which includes:

- ***cfg.samp_interval***: the time (single value) between each two consecutive data sample, in the unit of millisecond, calculated by reversing the sample frequency.
- ***cfg.epoch_twd***: a two values vector, containing the time window of the epoch (the first dimension of the 3-d data), in the unit of millisecond. e.g., if it is from -100ms to 1000ms, set it as [-100,1000]; (here is in the unit of millisecond). It must be must 0, in order to detect the stimulus onset. In the case of datasets used in this thesis work, the EEG signal is divided into epoch of 8000 ms, considering 5000 ms and 3000 ms after the stimulus onset, so this parameter is set to [-5000 3000].
- ***cfg.comp.name***: a cell variable containing the names of the components to decompose. In this project, three components are separated, namely 's', 'c', 'r'.
- ***cfg.comp.twd***: the time window where each component is supposed to occur, used to constrain the search of such components (and the C component latency). The determination of component time windows is mainly based on the pattern of ERP waveform, so such interval can be visually estimated (Figure 4.8).

In this case:

- The time window for *S component* is set from -2000 ms to 500 ms, relying on the fact that Readiness Potentials shows a detectable activity before the stimulus onset, especially in voluntary tasks, where there is an overt preparation stage for action.
- The time window of *C component* is set to be from 100 ms to 1500 ms based on the visual inspection of the data of the central component.
- The time window of *R component* is set from -300 ms to 300 ms: while for S and C the values of time window are relative to the stimulus onset, in this case they are referred to reaction time, justifying the negative value.

- ***cfg.comp.latency***: the latency information for the component one wants to separate. In general, the latency of S component is all-zero vector, because it is locked to the stimulus onset and the latency of R component is the vector of reaction times. The latency of C component should be set to be ‘unknown’ as it is to be estimated.

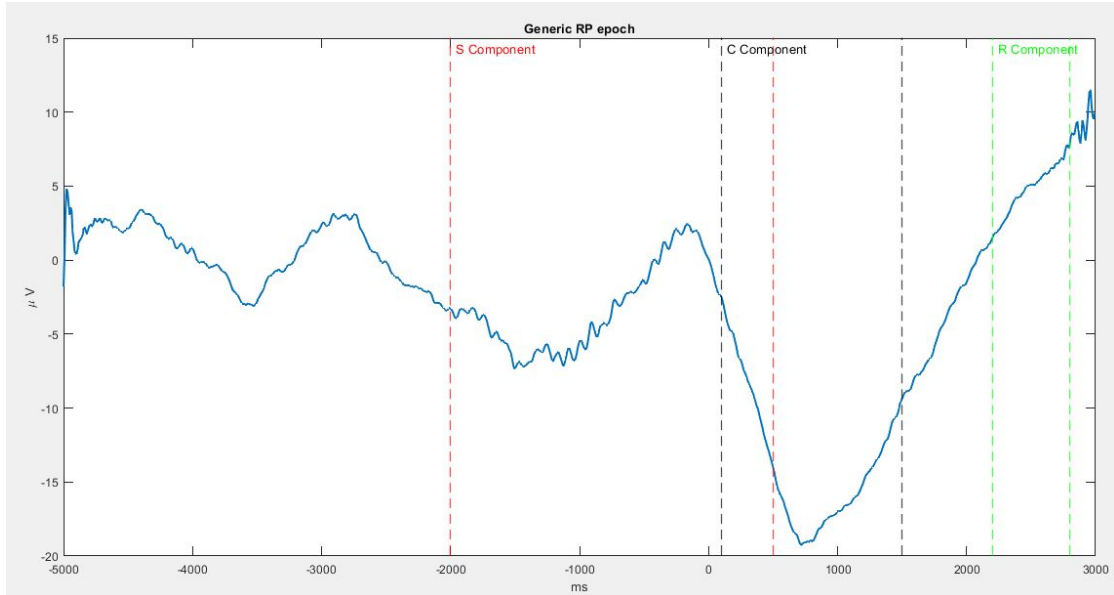


Figure 4.8: Single trial ERP signal referred to C3 channel, in which three components can be identified in the chosen time window.

RIDE algorithm returns a variable called ‘results’, where all of the outcomes are contained:

- ***erp***: the original ERP, obtained averaging the original single trials for each electrode, with the size of *epoch length x number of channels*.
- ***s***: S component separated by RIDE, with the size of *epoch length x number of channels*. S component is baselined with the mean values of the segment of [0-200 ms].
- ***c***: same as above. This C component is the latency-synchronized, which is different from the *c_sl* later (stimulus-locked averaged) in the following. Latency-synchronized means that all the single trials of C components are synchronized to the mean latency and the waveform is located at the most probable latency (here the median). C component is baselined on [0-200 ms] based on the assumption that there should not be significant activity in the early time window.

- **r**: same as above. This R component is synchronized to the reaction time and is put at the most probable reaction time (here the median).
- **s_sl**: the convention stimulus-locked average of S component (equal to s).
- **c_sl**: the conventional stimulus-locked average of C component (the blurred version).
- **r_sl**: the conventional stimulus-locked average of R component (the blurred version).
- **latency_c**: the latencies of C component for each single trial relative to the template of C component at the unit of millisecond.
- **latency_r**: the reaction times after subtracting the median (at the unit of millisecond). To retrieve the original RT, one can refer to results.latency0, third cell.
- **amp_s**: the amplitude of S component for each single trial and each single channel estimated by covariance between the S component and single trial after removal of other RIDE component. The size is *trial number x channel number*.
- **amp_c**: same as above.
- **amp_r**: same as above.
- **erp_new**: the reconstructed ERP by summation of 's','c' and 'r' which are the RIDE components located at the most probable latency.

4.3.4 Results and Plots

As shown in Figure 4.7, RIDE results are displayed in different types of plots, which focus on the time courses of the single components and the reconstructed ERP, allowing a detailed analysis of the single electrode behaviour and all electrodes together.

The dataset used to present the algorithm's results is *GF892070 - Voluntary task*.

RIDE components

In the following plots (Figure 4.9, 4.10, and 4.11), RIDE components are displayed for all electrodes: apart from some outlier channels, the channel seems to detect greater activity in the time window supposed to contain it.

In particular, for each component:

- **S component**, locked to the external stimulus, enhances the brain preparation activity in submitting the task, above all in the pre-supplementary motor area (pre-SMA), showing meaningful fluctuation around the stimulus onset.
- **C component** is directly correlated to the movement execution and shows highest amplitudes due to the activation of the primary motor cortex. It mainly occurs around 1000 ms after the stimulus onset, as expected when carrying out a voluntary task.
- **R component**, locked to the response, has very low amplitudes because of the nature of the task, which involves no real activity related to the response. It has a little higher amplitudes in the late signal because of the movement just executed, but it has practically no influence on the final ERP. In this work, R component is presented for the sake of completeness, but it can be omitted, as any possible combination of components can be considered in RIDE algorithm.

For clarity, Figure 4.12 shows separated components for channel C3, which should be one of the most involved electrodes in detecting brain activity related to the right hand movements.

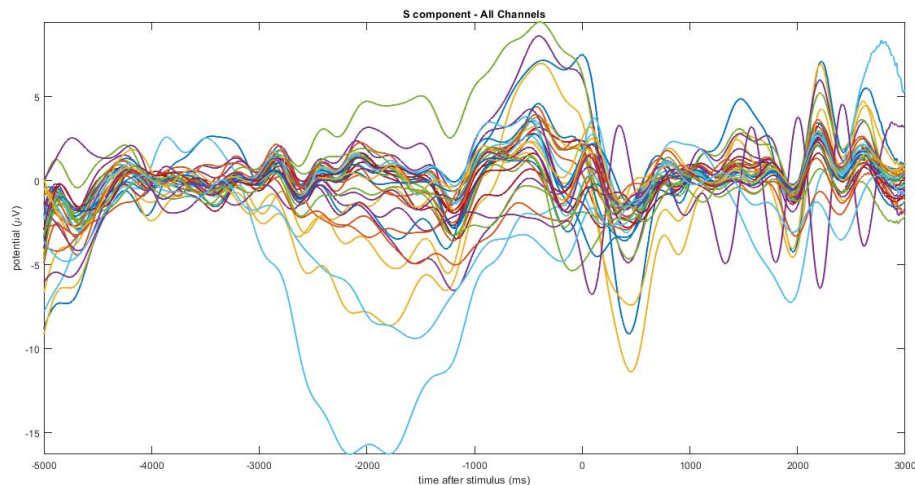


Figure 4.9: Illustration of the superposition of S component signals for the whole set of electrodes.

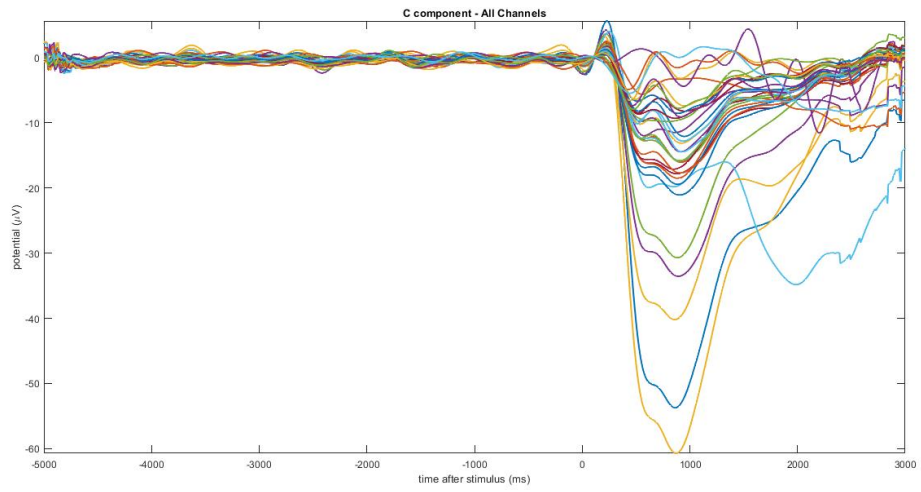


Figure 4.10: Illustration of the superposition of C component signals for the whole set of electrodes.

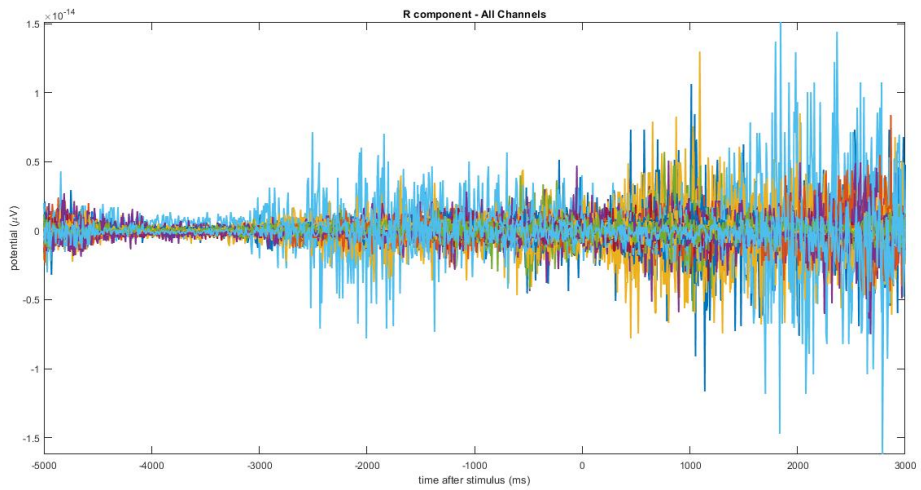


Figure 4.11: Illustration of the superposition of R component signals for the whole set of electrodes.

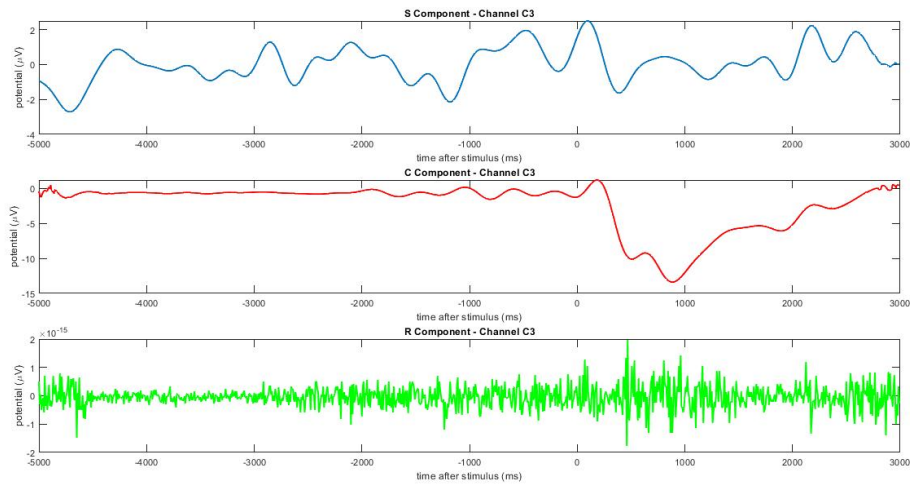


Figure 4.12: Separated components for channel C3.

Reconstructed ERPs

In the following plots, the final results of the jitter compensation method is shown. The reconstructed ERP is compared with the original one, obtained simply by averaging all epochs, without taking into account the trial-to-trial variability.

In Figure 4.13, the blue signals represents the resulting potential referred to the sample channel C3: as set out among the aims of the algorithm, the reconstructed ERP shows increased amplitudes with respect to the original one, avoiding the blurring and smearing effect which other jitter compensation methods may involve. Furthermore, every part of the signal is re-aligned to the marker which is locked to, proving the compensation of the delay which affected the original single trials.

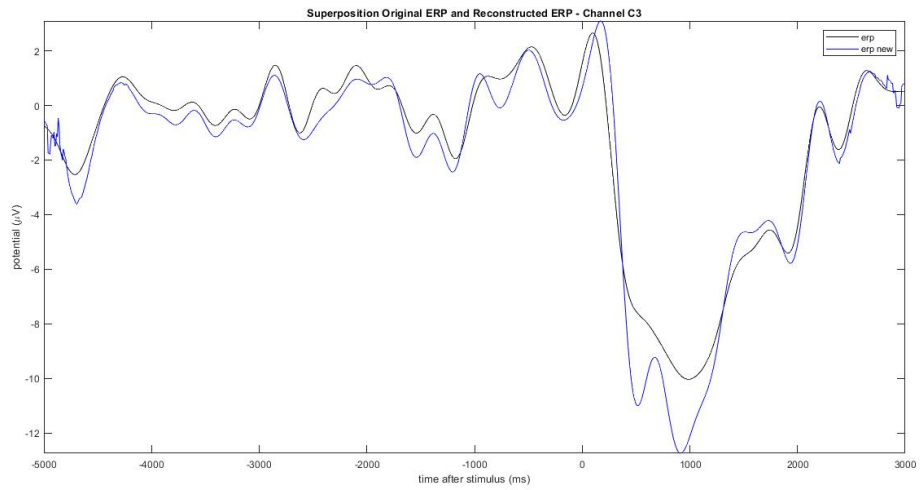


Figure 4.13: Illustration of the superposition of C component signals for the whole set of electrodes.

When considering all electrodes, the effect of amplitude increasing and correct jitter compensation is even more evident: as shown in Figure 4.14, all potentials follow the same pattern, with different amplitudes depending on the spatial distribution of the electrodes on the scalp.

The superposition of resulting RIDE components and reconstructed ERPs are shown for six channels (Figure 4.15), considering the mostly involved areas in the preparation stage and movement execution: as already pointed out, the component that has the greatest weight in the reconstruction of the ERP is the C component, relative to the movement execution, which has significant amplitudes in all the channels considered.

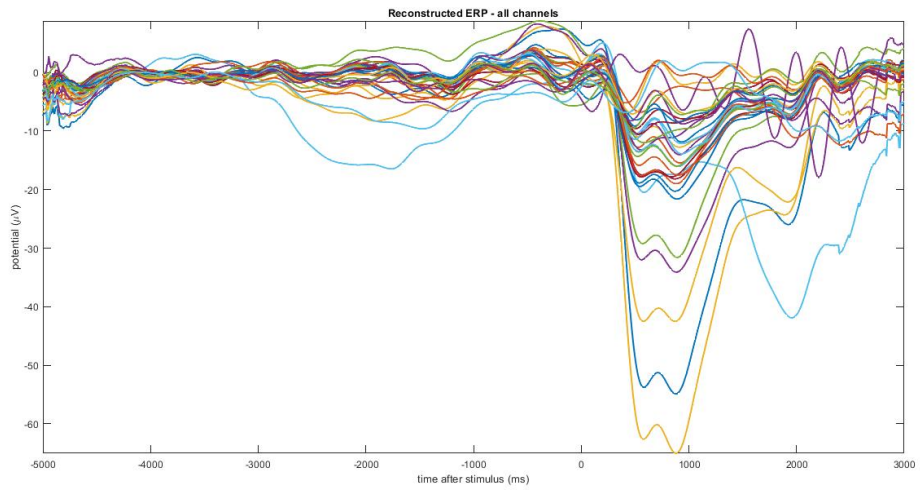


Figure 4.14: Illustration of the superposition of R component signals for the whole set of electrodes.

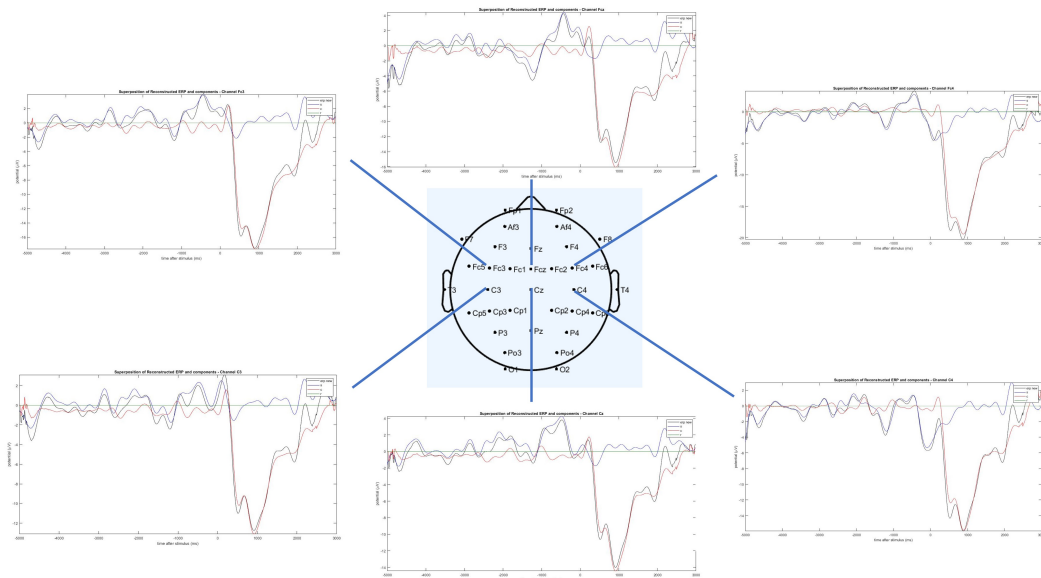


Figure 4.15: Separated components for channel C3.

4.3.5 Comparing Methods: Woody’s Method vs. RIDE Method

In order to assess if the RIDE method brings an effective improvement to the jitter compensation function already in use in the MRCPLAB plug-in, it was necessary to compare the results of the two methods, graphing the RP obtained in both cases.

For clarity in the representation, a channel selection was made, considering only seven electrodes placed in the brain areas involved in the tasks provided by the protocols.

Since the RP is detected over the Sensorimotor Cortex, including Pre-Motor and Motor Areas, and over the Somatosensory Cortex in the Parietal Lobe, the following channels are considered: *Cz, C3, C4, Fcz, Fc3, Fc4, Pz*. By averaging different combinations of ERP coming from the selected channels, one can obtain a RP representing a specific brain area, as indicated in Table 4.1.

Brain Area	Averaged Channels
Pre-Motor Area	Fcz, Fc3, Fc4
Motor Area	Cz, C3, C4
Median Rosto-Caudal Area	Cz, Fcz, Pz
Right Hemisphere Electrodes	C4, Fc4
Left Hemisphere Electrodes	C3, Fc3

Table 4.1: Different combinations of averaged RPs representing different areas of the brain.

Dataset GF892070 - Voluntary task

Although there is no appreciable difference in the amplitudes of the RP obtained with both methods, the signals resulting from the RIDE method follow a common pattern in the different areas of the brain, resulting more compact in the visualization (Figure 4.16 and Figure 4.17).

By superimposing the signals relative to the motor and pre-motor zone, it is possible to notice that the RIDE potential compensates with greater evidence the delay due to the trial-to-trial latency variability (Figure 4.18 and Figure 4.19).

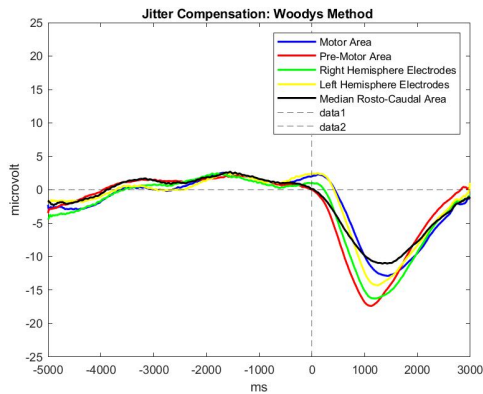


Figure 4.16: Jitter compensation: Woody's Method

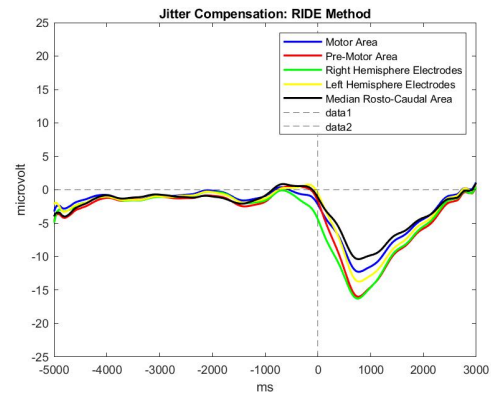


Figure 4.17: Jitter compensation: RIDE Method

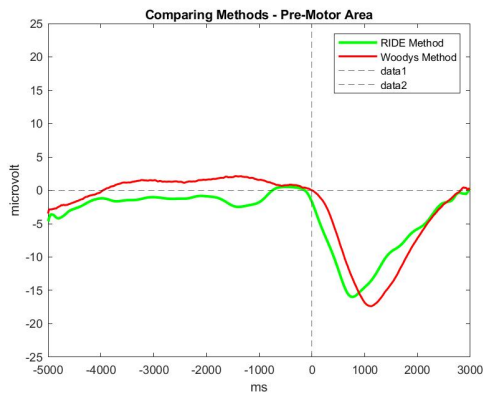


Figure 4.18: Superposition of methods: Pre-Motor Area

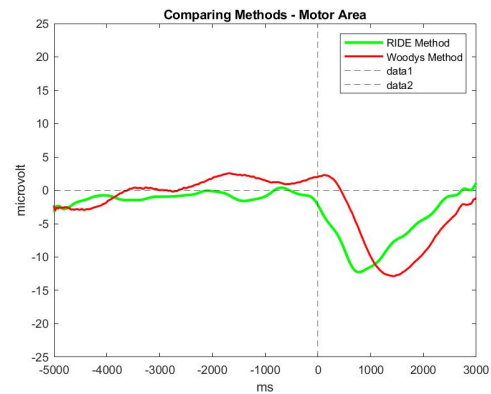


Figure 4.19: Superposition of methods: Motor Area

Dataset TC995011 - Voluntary task

This dataset highlights the advantages of the RIDE method over trial methods: it eliminates the blurring effect, increasing the signal amplitude and defining the waveform (Figure 4.20 and Figure 4.21).

Furthermore, as Figure 4.22 and Figure 4.23 Figure shows, the peak related to movement execution is re-aligned in the correct way.

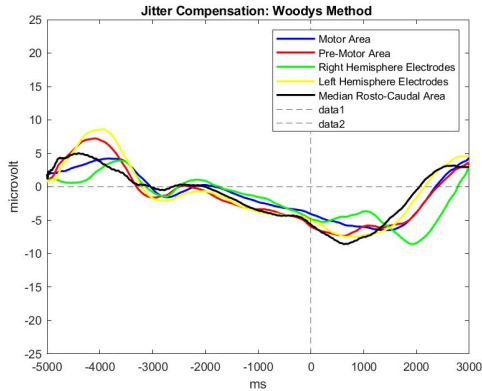


Figure 4.20: Jitter compensation: Woody's Method

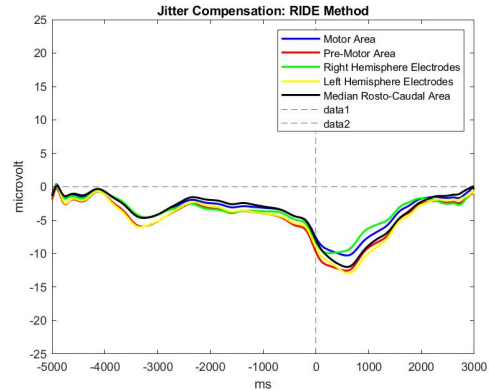


Figure 4.21: Jitter compensation: RIDE Method

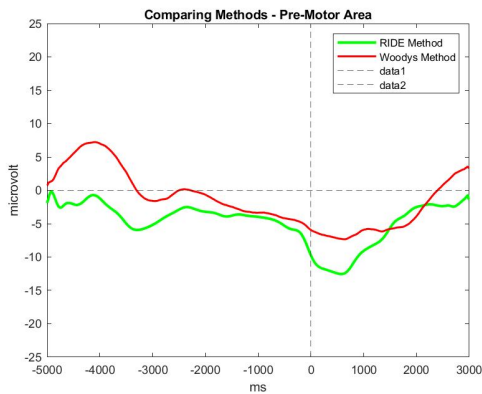


Figure 4.22: Superposition of methods: Pre-Motor Area

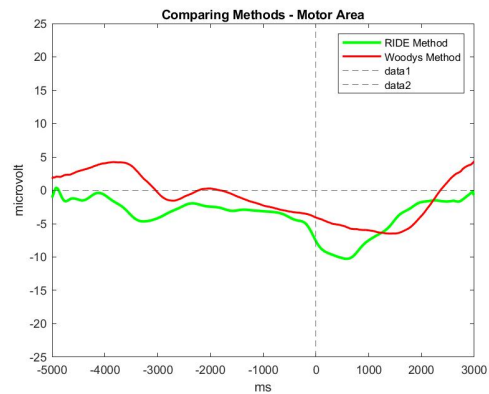


Figure 4.23: Superposition of methods: Motor Area

Dataset RB890071 - Semivoluntary task

As in the previous dataset, the comparison between Woody's and RIDE Method elicits the improved ability of the latter to get a RP signal.

The unusual waveform of the RP obtained with the previous method may be caused by an underperforming artifacts correction and noise removal: by separating components and re-aligning each component to each specific latency, RIDE manages to eliminate random noise and enhance only significant signal information (Figure 4.24 and Figure 4.25).

As Figure 4.26 and Figure 4.27 shows, RIDE ERP displays a visible peak related to the movement execution and better aligned to the stimulus with respect to the other ERP, even if a semivoluntary task requires the maximum amplitude to be around the onset, remembering that some improvements can still be made.

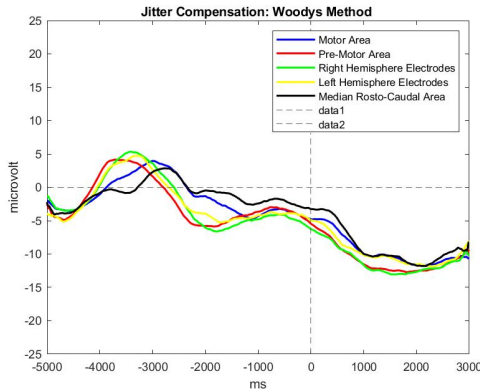


Figure 4.24: Jitter Compensation: Woody's Method

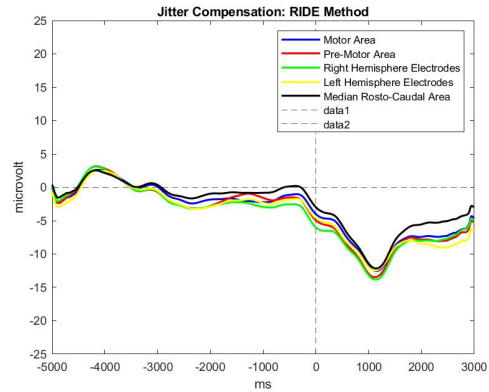


Figure 4.25: Jitter Compensation: RIDE Method

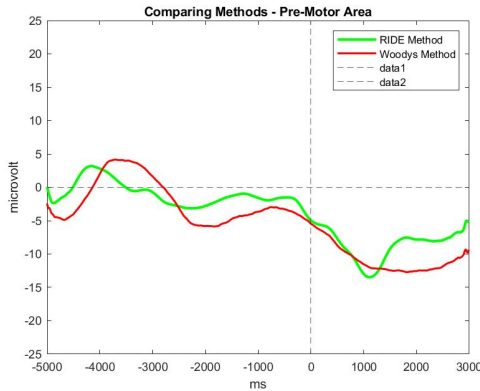


Figure 4.26: Superposition of methods: Pre-Motor Area

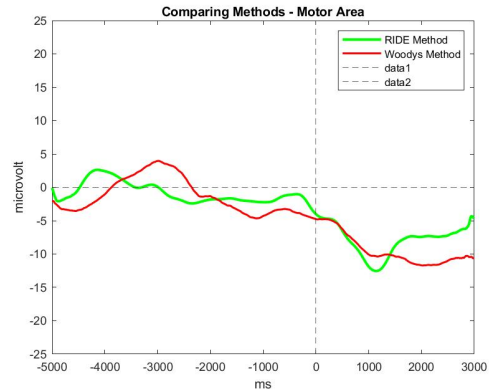


Figure 4.27: Superposition of methods: Motor Area

Dataset SD874070 - Semivoluntary task

As in the previous dataset, the new method for jitter compensation is able to elicit the component linked to the movement, which in the previous method seems to be attenuated and confused in the background noise (Figure 4.28 and Figure 4.29).

Averaged ERPs for the motor and pre-motor areas shows visible aligned peaks, closer to the stimulus onset, as one expects from a semivoluntary task (Figure 4.30 and Figure 4.31).

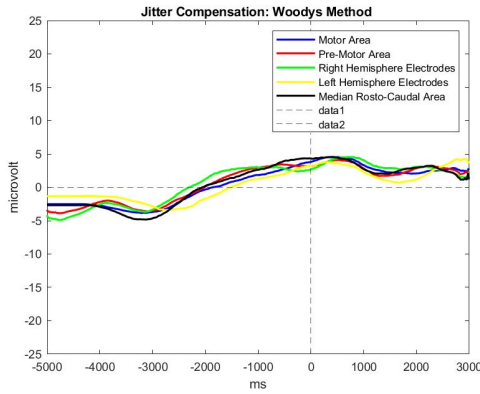


Figure 4.28: Jitter Compensation: Woody's Method

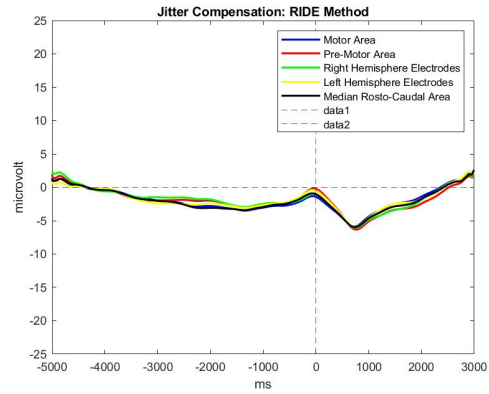


Figure 4.29: Jitter Compensation: RIDE Method

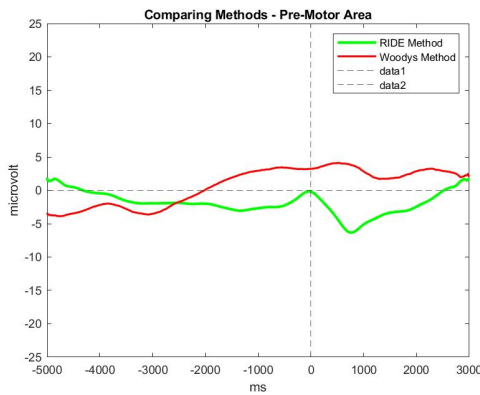


Figure 4.30: Superposition of methods: Pre-Motor Area

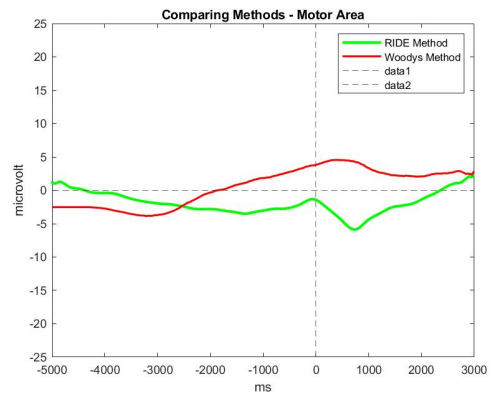


Figure 4.31: Superposition of methods: Motor Area

Dataset SP880071 - Involuntary task

Since the task performed is involuntary, aimed at stimulating the patellar reflex with a gavel, the expected RP is flat, with no cerebral awareness or voltage peak related to movement.

RIDE signal best meets these requirements, as shown in Figure 4.32 and Figure 4.33, both in the pre-motor and motor area (Figure 4.34 and Figure 4.35)

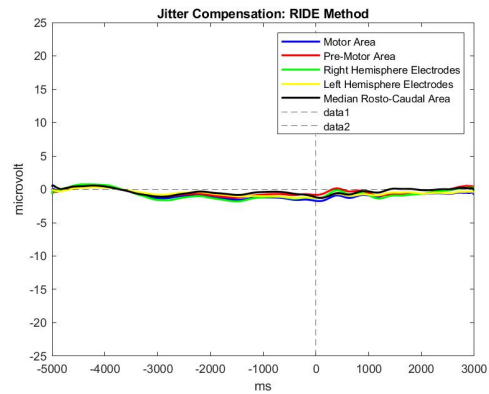
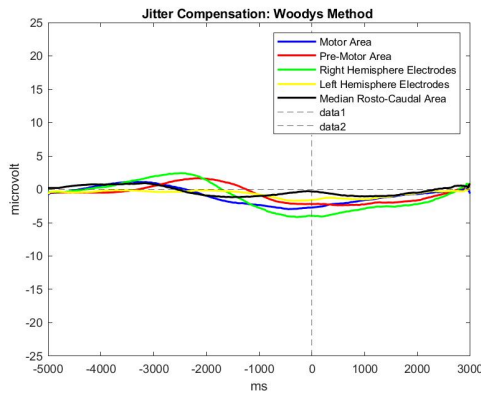


Figure 4.32: Jitter Compensation: Woody's Method

Figure 4.33: Jitter Compensation: RIDE Method

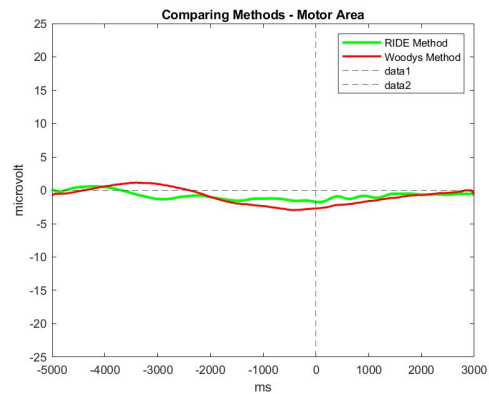
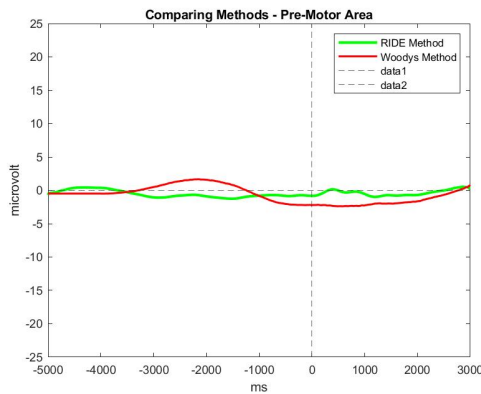


Figure 4.34: Superposition of methods: Pre-Motor Area

Figure 4.35: Superposition of methods: Motor Area

Dataset AP996111 - Involuntary task

As with the previous dataset, it is expected that the ERP signal related to an involuntary task will not have visible fluctuations. In this case, RIDE is able to detect a peak, even if small in amplitude, probably caused by an adaptation of the subject in the different trials (Figure 4.38, Figure 4.39, Figure 4.38 and Figure 4.39)

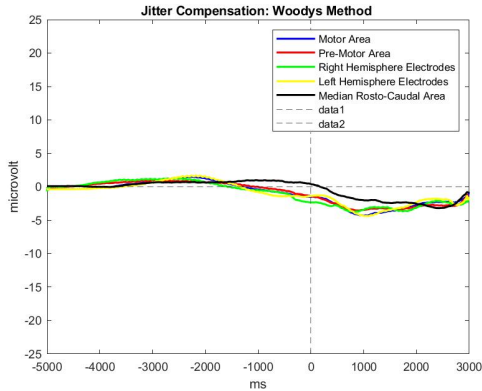


Figure 4.36: Woody's Method

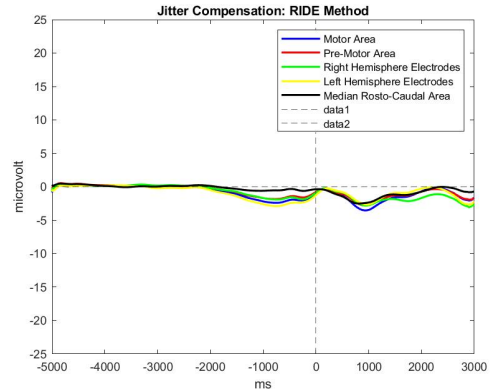


Figure 4.37: RIDE Method

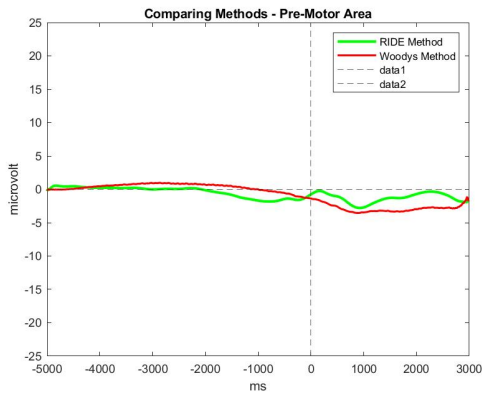


Figure 4.38: Superposition of methods: Pre-Motor Area

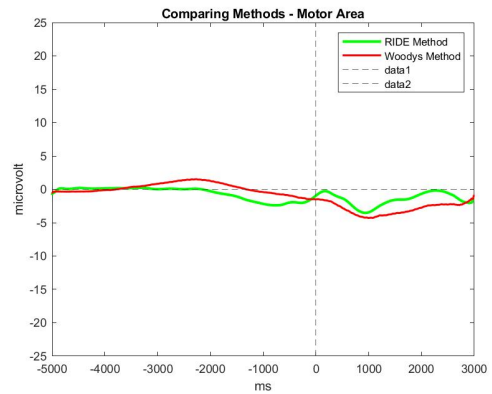


Figure 4.39: Superposition of methods: Motor Area

4.3.6 Combining Methods: Woody's and RIDE in cascade

Although RIDE gave the expected results, later attempts were carried out to further improve the effectiveness of the jitter compensation algorithm.

The idea is to insert in the MRCPLAB plug-in an algorithm that includes the two methods (Woody's and RIDE) in cascade: the signal resulting from the compensation of latency variability with Woody's method is given as input to the RIDE method, in order to take advantage from the strengths of both methods.

In the following, the results of this hybrid algorithm will be presented: for some

datasets examples, charts show the signal deriving from the average of different electrodes ERPs for each zone (as described in the Table 4.1) and the differences with the two methods taken individually are highlighted for the motor area, more involved in the execution of the task.

Dataset LF864071 - Voluntary task

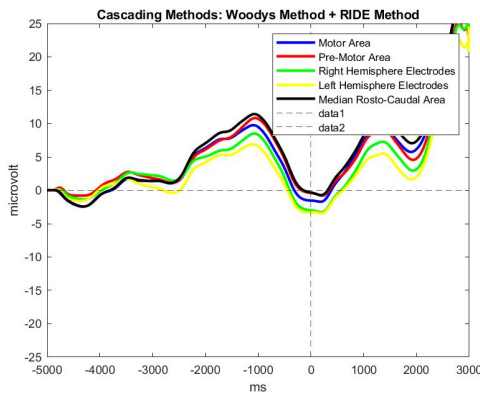


Figure 4.40: Methods in cascade

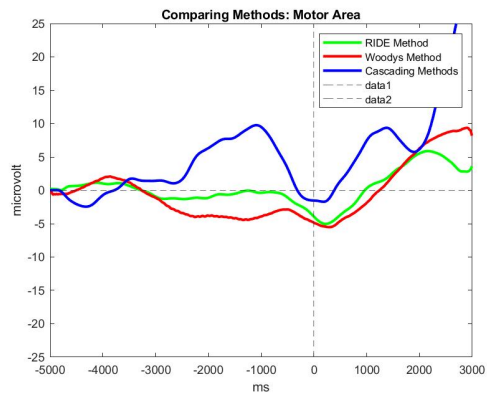


Figure 4.41: Superposition of Methods: Motor area

Dataset GO862071 - Semivoluntary task

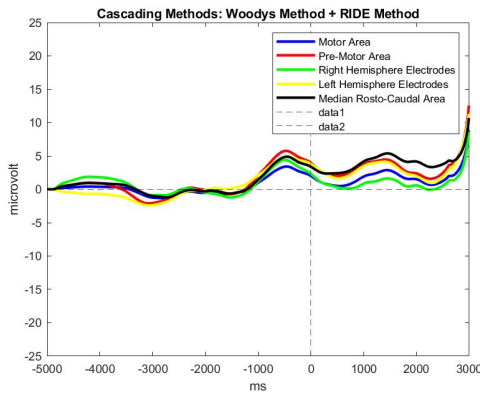


Figure 4.42: Methods in cascade

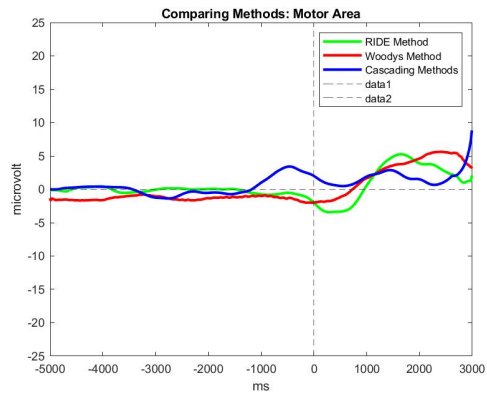


Figure 4.43: Superposition of Methods: Motor area

Dataset RG865070 - Involuntary task

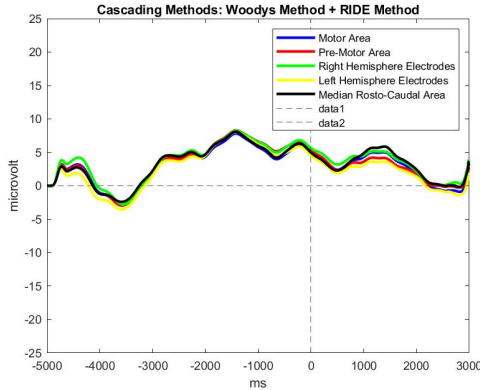


Figure 4.44: Methods in cascade

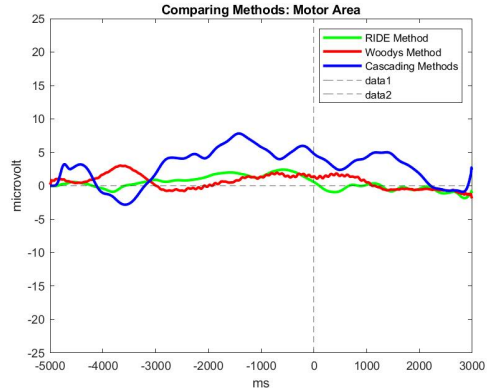


Figure 4.45: Superposition of Methods: Motor area

From the graphs reporting the trend of the averaged signal obtained in the single areas, it is evident that all the ERP are in agreement in the pattern (Figure 4.40, Figure 4.42 and Figure 4.44).

Nevertheless, looking at the graphs obtained comparing the three methods, it is clear that the use of Woody's and RIDE methods in cascade does not bring any improvement to the RP waveform (Figure 4.41, Figure 4.43 and Figure 4.45). Therefore, RIDE is confirmed to be the method that, depending on the type of task, is able to bestly elicit the different components of the signal, whether they are related to the preparation and execution of the movement.

In order to improve the previous method, another attempt was made, based on the weaknesses found with the Woody's algorithm.

As already described in Section 4.2.1, one issue about Woody's method is the dependency on Fcz channel latency, since the shift applied to every epoch in order to re-align it is calculated for the epochs of the channel Fcz and applied in the same way to all the corresponding epochs of the other channels.

Thus, the idea is to insert the two methods in cascade, making in this sense an adjustment to the Woody's method: instead of taking as a reference the only Fcz signal for all electrodes, four zones have been defined, within which the shifts applied to the epochs are calculated referring to four different reference electrodes. The selected areas are the frontal lobe, the parietal with occipital lobes, the right temporal lobe and the left temporal lobe, represented respectively by the electrodes Fcz, Pz, T4 and T3. Table 4.2 reports reports the zoning and, for each zone, the

channels whose RP has been averaged.

Brain Area	Averaged Channels
Frontal Lobe	Fp1, Fp2, Af3, Af4, F7, F3, Fz, F4, F8, Fcz, Fc5, Fc1, Fc2, Fc6, Fc4, C3, Cz, C4, Cp3, Cp5, Cp1, Fc3, Cp2, Cp6, Cp4
Parietal and Occipital Lobe	Po3, O2, Po4, P3, Pz, P4, O1
Right Temporal Lobe	T4
Left Temporal Lobe	T3

Table 4.2: Brain zoning applied to Woody’s Method as a reference for epoch realignment.

Dataset TC995011 - Voluntary task

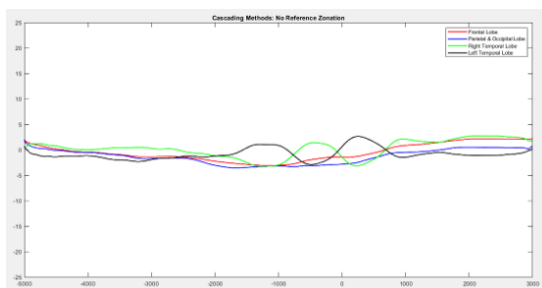


Figure 4.46: Methods in cascade

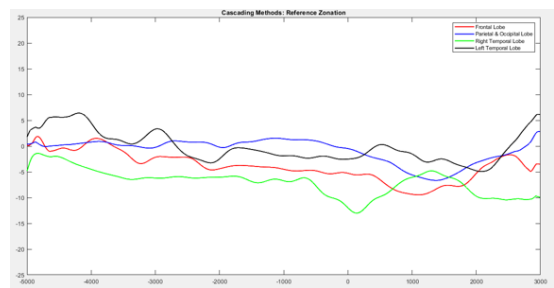


Figure 4.47: Superposition of Methods: Motor area

Dataset AL858070 - Semivoluntary task

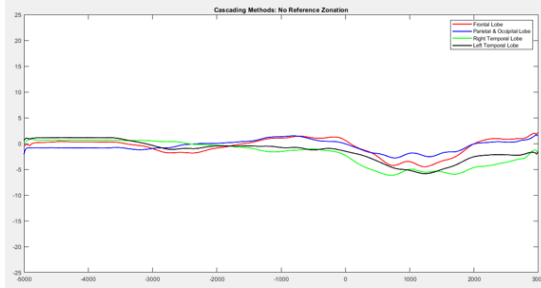


Figure 4.48: Methods in cascade

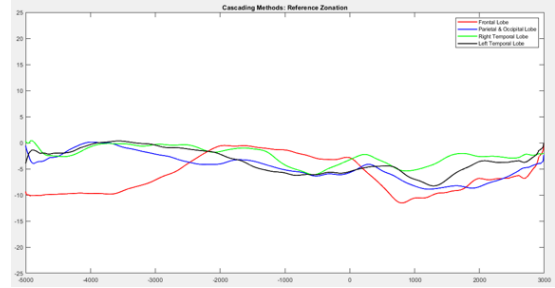


Figure 4.49: Superposition of Methods: Motor area

Dataset SP880071 - Involuntary task

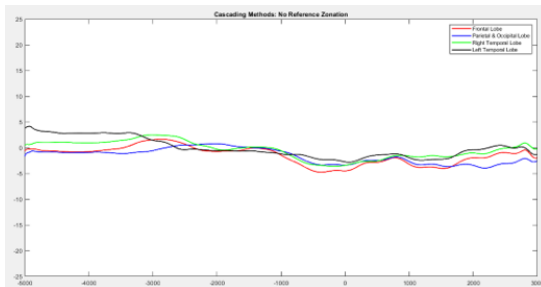


Figure 4.50: Methods in cascade

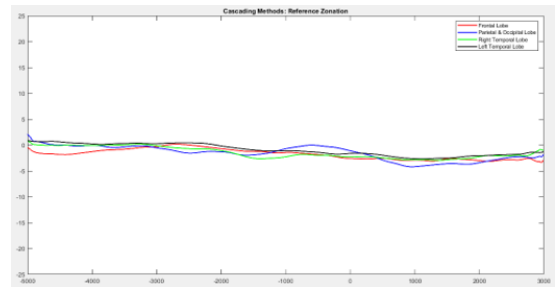


Figure 4.51: Superposition of Methods: Motor area

As expected, in general, comparing the RPs obtained with the original Woody's and RIDE cascade method and the Woody's method modified with several electrodes as a reference for epoch shifting (always cascading with RIDE), it can be noted that the latter is the best method, depending on the tasks considered. Actually, the obtained RPs bestly elicit the preparation and the movement execution stage, comparing with the first approach which smears the waveform and confuses relevant components.

4.4 Discussion

The compensation of trial-to-trial latency variability is one of the main issues in the pre-processing chain of a biological signal. The well-known problem of jittering, actually, is a timing misalignment of the EEG epochs, due to small changes in the brain times across all the trials and movements' onsets timing detection, which results in blurred and attenuated waveforms when averaging epochs.

Within the main project started before this thesis work, the problem has already been addressed, providing as a solution the Woody's method. However, this method provides for some limitations, such as (1) the identification of a single component on which carrying out the correction of the latency and (2) the dependence from the Fcz channel estimated latencies, that are applied in the same way to all the corresponding epochs of the other channels.

The novelty of the RIDE method consists in the separation of the ERP in components with different latencies, related to the stimulus, the response or neither, and in the re-alignment of the waveforms of each component, synchronizing them to their most probable latency. In this way, the reconstructed ERPs show enhanced amplitudes, deriving from the average of synchronized waveforms, and richer structure, avoiding the blurring effect due to trial-to-trial latency jitter.

Comparing the results obtained with this innovative method with those obtained with the previous Woody's method, it is possible to appreciate the advantages of the RIDE algorithm: depending on the task performed by the subject, ERPs waveforms are better defined and synchronized to the stimulus onset, allowing the distinction among different stages of the task, such as the brain preparation for the movement (when it is required) and the execution of the movement itself, highlighting the peaks and characteristic fluctuation thanks to the de-blurring effect of this jitter compensation algorithm.

An alternative solution has been tested, which combines the two methods in cascade: the signal resulting from the compensation of latency variability with Woody's method is given as input to the RIDE method. However, this method did not give the expected results because, in most of the datasets analyzed, it has worsened performance compared to the previously implemented RIDE method, which is confirmed to be the best among the three analyzed algorithms.

Another attempt was made by maintaining the cascading structure of the latter algorithm, starting from one of the weaknesses of the Woody's method, that is the dependence on the Fcz channel for the latencies compensation of different epochs. The novel algorithm provides that the electrodes are grouped according to the brain

areas to which they belong and therefore have four different reference channels for the realignment of the epochs, instead of taking the only Fcz signal for all channels. The selected areas are the frontal lobe, the parietal with occipital lobe, the right temporal lobe and the left temporal lobe, represented respectively by the electrodes Fcz, Pz, T4 and T3.

Comparing the two novel algorithms which both require the cascade of the Woody's method and RIDE method, better results can be observed when adjustment are made to the Woody's method: in this case, the waveform is well defined, eliciting all the RP's components, with respect to the simple cascade of the original Woody's and RIDE method, which provide attenuated amplitudes and confused components, with poor alignment to the onset.

Relying on the obtained results, the MRCPLAB plug-in has been updated by including the two methods for jitter compensation that showed the best results, namely RIDE method and the cascade of Woody's method (the optimized version) and RIDE method.

4.4.1 Limitations and Future Challenges

RIDE method is designed for avoiding the smearing effect or attenuated amplitudes resulting from the conventional average of different trials, separating components and re-synchronizing them to their own latencies.

Actually, in this case, the obtained signals show enhanced amplitudes and richer waveforms, but some critical issues can be highlighted and possibly improved in the future:

- i. The algorithm allows you to choose how many components the signal must be divided; in this case, the selected components are three, starting from the assumption that, in general, there are three types of components (stimulus-locked component, response-locked component, neither-nor component). This could inevitably be a simplification of the ERP structure, as there could be several components, especially C components, that have variable latencies independently of each other and can contribute to a more accurate reconstruction of the signal.
- ii. As well as the choice of the number of components, also the definition of a specific time window for each component introduces a certain degree of subjectivity in the algorithm, as they are assumed simply by visual inspection of the average ERP waveforms, requiring prior knowledge about the signal and the temporal characteristics of the components.
- iii. The latency estimation of the "neither-nor" C component, which is supposed to be unknown, is performed by cross-correlation between epochs, which may

be affected by background noise that may lead to mis-correlations. Such issue can be alleviated by increasing the number of the trials or by enhancing the signal-to-noise ratio through careful pre-processing. [27]

Chapter 5

ERP Temporal Filtering

Temporal filtering aims to remove or attenuate frequencies within the raw signal, improving the signal-to-noise ratio and the signal visualization.

Typically, EEG signals are filtered with a high-pass filter with cut-off frequency from 0.1 Hz to 1 Hz for eliminating slow drifts and with a low-pass filter for cutting-off frequencies greater than 40-50 Hz.

In this case, the raw signal is already filtered between 0.1 Hz and 40 Hz, before any pre-processing step, while importing the file ASCII to EEGLAB.

5.1 Methods and Results

In the case of Readiness Potentials, it is important to obtain a clear, smooth and interference-free waveform, in order to elicit the most significant components of the signal (related to the preparation and execution of the movement) and allow a more accurate classification. The tricky thing is to decide which frequencies are of interest and which are noise: in this perspective, the Power Spectral Density (PSD) of the RP has been computed, then zooming on the frequencies between 2 Hz and 32 Hz for better analysis (Figure 5.1 and Figure 5.2).

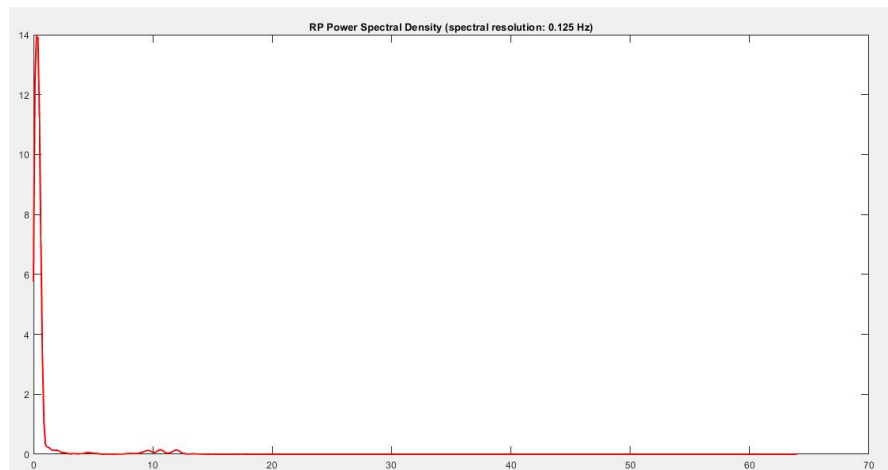


Figure 5.1: RP power spectral density (PSD) computed with spectral resolution of 0.125 Hz.

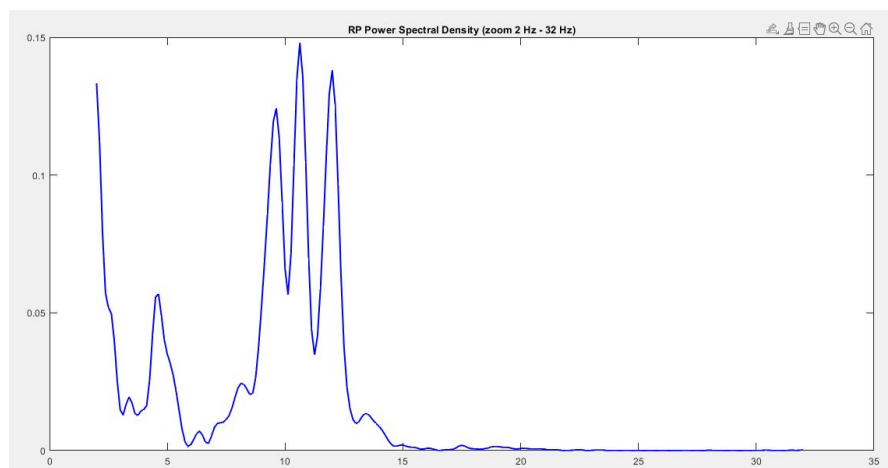


Figure 5.2: RP power spectral density (PSD) zooming on frequencies 2-32 Hz.

The power spectral density computed on the obtained RP shows two main peaks: the first one around 3 Hz and the second one at higher frequencies, from 8 Hz to 10 Hz. Since the peak at 3 Hz is what the literature claims to be related to the frequency of the RP occurrence, it is deduced that the second one is the result of high frequency fluctuations, which can be eliminated. Therefore, a low-pass filter with a cut-off frequency of 3 Hz is applied to the signal.

The first issue is about what type of filter should be applied:

- **FIR (Finite Impulse Response) filter**, a Linear Time-Invariant (LTI)

causal system whose impulse response, as the name suggests, is of finite duration.

The main advantages are the possible linear phase (if the filter is designed with a symmetric or antisymmetric coefficients sequence), which implies no distortion of the output signal, the stability and the causality, for which no feedback is required, because producing the output needs only a certain number of inputs.

As a disadvantage, with equal performances, a FIR filter requires a higher order than the IIR filter and, consequently, output samples will be affected by a greater delay with respect to the input signal (the delay in sample is equal to the order of the filter used).

- **IIR (Infinite Impulse Response) filter**, which as an impulse response which does not become exactly zero past a certain point, but continues indefinitely. This filter is self-regressive and recursive: in order to generate the output, in addition to the input values, some output values are needed, which are previously produced. Together with the advantage over the FIR filter described above, IIR filters have some disadvantages, among which the most important is the non-linear phase, that produces a distortion not easily predictable a priori: in order to compensate for the distortion introduced by the filter, an anticausal or double pass filtering should be applied.

The choice of the filter to be used was validated by observing the time course of a generic epoch without any kind of pre-processing (only filtered at the beginning of the chain between 0.01 and 40 Hz), to which the same epoch was superimposed, firstly filtered with a FIR filter of order 25 and secondly with an IIR filter of order 9, as shown in Figure 5.3 and Figure 5.4.

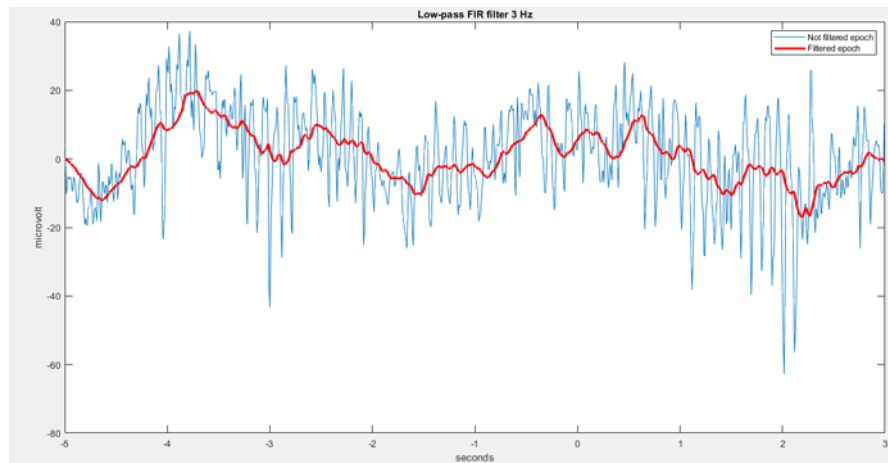


Figure 5.3: EEG epoch before any kind of processing, with the superposition of the same epoch filtered at 3 Hz with a FIR filter (order 25).

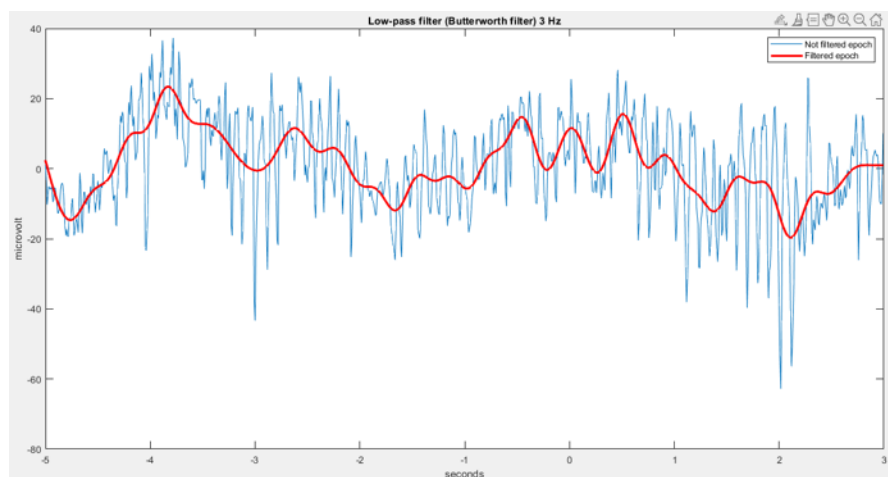


Figure 5.4: EEG epoch before any kind of processing, with the superposition of the same epoch filtered at 3 Hz with a IIR filter (order 9).

IIR filter of order 9 has been selected, as it has better performance with a lower order, which implies less delay of the output samples.

The second issue concerns the positioning of the filter within the pre-processing chain: inserting it before or after the epoch calculation can lead to significant differences in the results of the signal processing operations. In particular, jitter compensation may be affected by filtering: for this reason, RIDE method is applied to a dataset as example (GF892070), comparing the results of such operation when

no filters are inserted and with the implementation of a 3 Hz low-pass filter before epoch calculation, then before jitter compensation (Figure 5.5 and Figure 5.6).

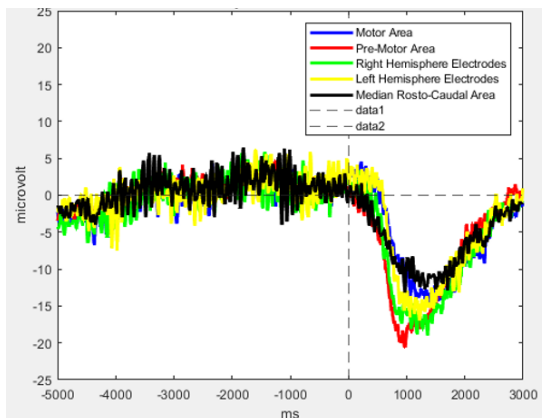


Figure 5.5: Jitter compensation applying RIDE method with no temporal filtering.

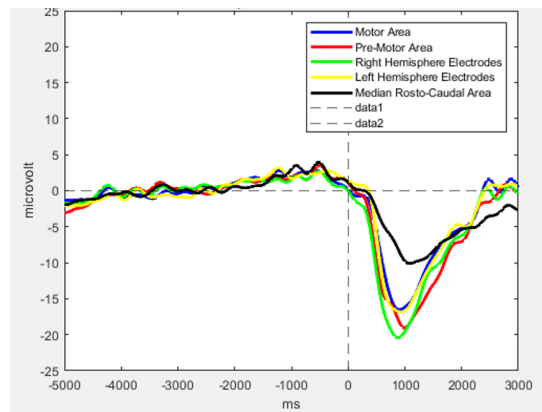


Figure 5.6: Jitter compensation applying RIDE method with a 3 Hz low-pass filter inserted before epoch calculation.

As expected, the IIR filter inserted before the epoch calculation corrupts the results of the jitter compensation.

Averaged ERPs referred to some brain areas seem not to match the corresponding signals obtained without the insertion of the 3 Hz filter: the latter seem to be more aligned to the onset stimulus and have less evident deviations than the ERPs obtained after filtering.

5.2 Discussion

Time filtering is one of the most important steps in processing EEG signals. In this work, after identifying the predominant frequencies in the signal, two issues were faced: the choice of the type of filter to be applied (if FIR or IIR filter) and the position of the filtering operation within the pre-processing chain.

After selecting as the most suitable filter the IIR filter of order 9 with cut-off frequency at 3 Hz, the signal was filtered before the division into epochs: the subsequent jitter compensation operation has a lower performance than the same operation performed with the unfiltered signals.

It's important to keep in mind that filtering changes data and this should be considered while interpreting the results, unless filtering is avoidable.

As demonstrated by study of Vanrullen, actually, the onset latency in the ERP can

be affected by tens to hundreds of milliseconds due to smoothing effects of low-pass filtering, that arises most prominently with the use of non-causal filters, due to backward filtering, as the implemented IIR filter is [30]. As already highlighted, this issue has an effect on the next steps of the pre-processing chain, which can lead to false interpretations in ERP studies.

In addition, observing the spectral power density of the signal, it has a relevant peak around 10 Hz: it can be concluded that in the higher frequency oscillations, between 8 Hz and 10 Hz, there is a high information content, useful to synchronise the epochs. The jitter compensation function, in fact, operates by calculating the cross-correlation between different epochs: it is possible that the presence of components at a higher frequency than the characteristic frequency of the RP is necessary for an efficient correlation between epochs, then accurate jitter compensation.

The reached compromise is the integration of a low pass filter with 20 Hz of cut-off frequency before computing the division in epochs, so as to keep intact the predominant frequencies in the signal. Subsequently, the "smooth" function is applied to jitter compensation results, which equals a low-pass filter at 1.28 Hz: this filter is used in the display of averaged ERP resulting from jitter compensation, as the last operation of the pre-processing chain.

Figure 5.7 and Figure 5.8 shows the results of the jitter compensation with a 20 Hz filter applied and then with the 'smooth' function applied after filtering.

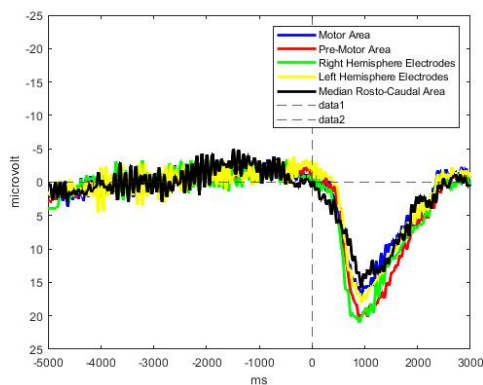


Figure 5.7: Jitter compensation applying RIDE method with 20 Hz low-pass filter before the epoch calculation.

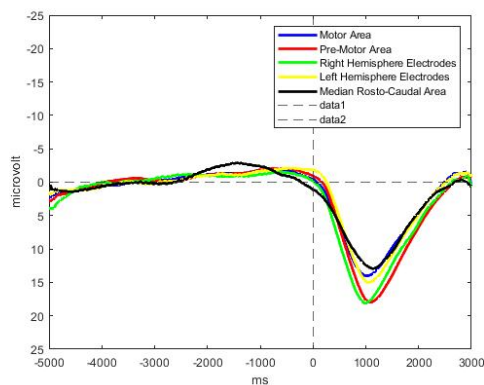


Figure 5.8: Jitter compensation applying RIDE method with a 20 Hz low-pass filter inserted before epoch calculation and 'smooth' function applied in the end for the visualization.

The MATLAB function *smooth.mat* smooths the input data using a moving average filter.

The moving average filter is a simple low-pass FIR (Finite Impulse Response) filter, which takes M samples of input at a time and computes the average in order to produce a single output point. As the span, namely the number of M sample, increases, the smoothness of the output increases. In this case, since the RP sampling frequency is 128 Hz and the span is set to 100, the result is a low-pass filter with a cut-off frequency equal to 1.28 Hz.

The implemented solution, that is to insert a low-pass filter at 20 Hz before the epoch calculation and to use the function "smooth" after the jitter compensation, allows to obtain both the wished performances in the pre-processing operations and a clear representation of the signal, which can be easily used later by machine learning algorithms.

Chapter 6

Conclusions and Ideas for the Future

This thesis work focuses on some steps of the pre-processing chain, in particular the Jitter Compensation and the ERP Temporal Filtering, in order to improve the quality of the obtained Readiness Potential (RP), allowing a more accurate classification.

With regard to jitter compensation operation, it can be concluded that the reconstructed ERPs obtained with RIDE method show enhanced amplitudes, deriving from the average of synchronized waveforms, and richer structure, avoiding the blurring effect due to trial-to-trial latency jitter. Some limitations are linked to (1) the choice of the number of components and the definition of a specific time window for each component, which introduce a certain degree of subjectivity in the algorithm, and (2) the latency estimation of the "neither-nor" C component, which may be affected by background noise that may lead to some errors in the cross-correlation.

For what concerns the temporal filtering, it can be noted that, after the implementation of a 3 Hz low-pass filter, the jitter compensation has lower performances than the same operation performed with the unfiltered signals. Actually, the jitter compensation function operates by calculating the cross-correlation between different epochs: the presence of components at a higher frequency is necessary for an efficient correlation between epochs, then accurate jitter compensation. However, it's important to keep in mind that filtering changes data and this should be considered while interpreting the results, unless filtering is avoidable.

6.1 Case study on a patient with Hemiplegia

Once improved the pre-processing pipeline, a key study was conducted on hemiplegic patients, in order to understand the presence of the LRP and its features in the contralateral side to the plegic limb in hemiplegic subjects.

The protocol involves both unimanual and bimanual voluntary tasks. In both cases, a comparison was made between right and left channel of the pre-motor area (Fc3 and FC4), linked to the intention to move, and the motor area (C3 and C4), related to the execution of the movement.

As expected, in the right unimanual task (Figure 6.1 and Figure 6.2), both areas show greater activity in channels Fc3 and C3, in the contralateral hemisphere with respect to the right limb, due to the programming and preparation stage for the pre-motor area and the movement execution for the motor area.

For the bimanual task (Figure 6.3 and Figure 6.4), in hemiplegic patients was asked to make an effort just imagining the execution of the task with the impaired limb. As a result, we found that, even with the impaired left limb, the RP related to channel Fc3 almost equals the one of channel Fc4, highlighting the presence of intention and motor programming even in the hemiplegic limb. For what concerns the motor area, the contralateral channel to the impaired limb shows smaller amplitudes because the movement isn't actually accomplished, but we can conclude that both imagining and performing a movement elicit the same early Readiness Potential in the pre-motor area, and two different later RP in the motor area proving that the motor intention is preserved in both sides even though obviously the execution is compromised in the plegic side.

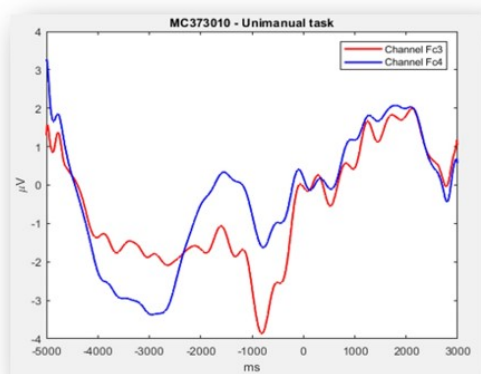


Figure 6.1: RP from channels Fc3 and Fc4 while performing Unimanual task.

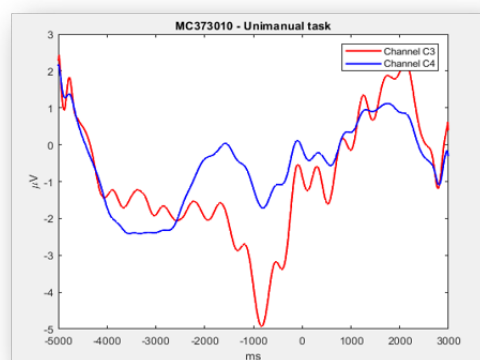


Figure 6.2: RP from channels C3 and C4 while performing Unimanual task.

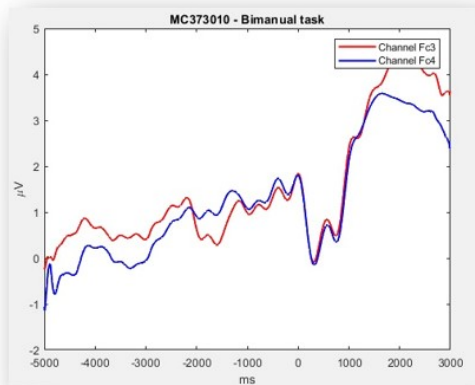


Figure 6.3: RP from channels Fc3 and Fc4 while performing Bimanual task.

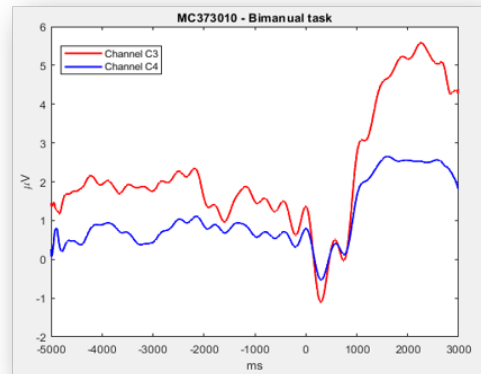


Figure 6.4: RP from channels C3 and C4 while performing Bimanual task.

Since MRCPLAB plugin and in particular the RIDE method for jitter compensation has been designed and tested on healthy subjects, we wanted to verify if this method had optimal results even with signals from pathological subjects. The test gave a positive result (Figure 6.5), as, again, RIDE manages to avoid the blurring effect introduced by averaging, to re-align the peak to the EMG onset and to enhance the signal amplitude.

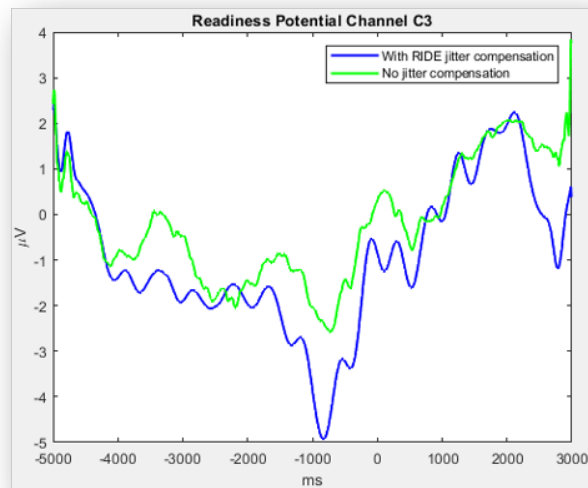


Figure 6.5: Readiness Potential from a hemiplegic subject (Channel C3) with RIDE jitter compensation (blue) and no jitter compensation applied (green).

Despite the jitter compensation gives good results, an effort must be made in the future by improving some steps of the pre-processing chain, in order to adapt it to the increased difficulty of signals from pathological subjects. In particular, improvements can be done about the artifact correction, as the signals from pathological subjects are on average noisier and rich in artifacts, and the detection of the EMG onset that, for the same reason, the currently present algorithm struggles to recognize correctly.

Such improvements are left to future researchers in order to obtain a BCI that can recognize minimal states of consciousness even when the patient shows no overt signs of awareness.

Bibliography

- [1] G. Brunetti. *La coscienza, alla ricerca di una propria identità*. 2020. URL: <http://www.neuroscienze.net/la-coscienza-alla-ricerca-di-una-propria-identita/> (cit. on p. 2).
- [2] D. Chalmers. *The Blackwell Companion to Consciousness*. Ed. by M. Velmans and S. Schneider. Blackwell Publishing Ltd, 2007 (cit. on p. 2).
- [3] M. Manfredi. *La coscienza e i suoi fondamenti biologici*. Treccani, 2010 (cit. on p. 3).
- [4] A. G. Casali et al. «A Theoretically Based Index of Consciousness Independent of Sensory Processing and Behavior». In: *Science Translational Medicine* 5 (Aug. 2013) (cit. on p. 5).
- [5] Istituto Superiore di Sanità. *Coma*. 2021. URL: <https://www.issalute.it/index.php/la-salute-dalla-a-alla-z-menu/c/coma?highlight=WyJkaWFhZXRlIl0=#sintomi> (cit. on p. 5).
- [6] C. Di Perri, L. Heine, E. Amico, A. Soddu, S. Laureys, and A. Demertzi. «Technology-based assessment in patients with disorders of consciousness». In: *Ann Ist Super Sanità* 50 (2014), pp. 209–220 (cit. on pp. 5, 8–10, 12, 14).
- [7] K. Maiese. *Vegetative State and Minimally Conscious State*. MSD Manual, 2020 (cit. on p. 6).
- [8] K. Maiese. *Minimally Conscious State*. MSD Manual, 2020 (cit. on p. 6).
- [9] K. Maiese. *Locked-in Syndrome*. MSD Manual, 2020 (cit. on p. 6).
- [10] T. Giacino Joseph, C. Schnakers, D. Rodriguez-Moreno, K. Kalmar, N. Schiff, and J. Hirsch. «Behavioral assessment in patients with disorders of consciousness: gold standard or fool’s gold? Progress in brain research». In: 177 (4) (2009), pp. 33–48 (cit. on p. 6).
- [11] S. Jain and L. M. Iverson. *Glasgow Coma Scale*. National Library of Medicine, 2021 (cit. on p. 7).

- [12] Margherita Urso. «Sviluppo di un metodo per la rimozione automatica e manuale degli artefatti per una BCI per pazienti non responsivi». MA thesis. Torino: Politecnico di Torino, 2021 (cit. on p. 7).
- [13] A. Shiel, S. A. Horn, B. A. Wilson, M. J. Watson, M. J. Campbell, and D. L. Mclellan. «The Wessex Head Injury Matrix (WHIM) main scale: a preliminary report on a scale to assess and monitor patient recovery after severe head injury». In: *Clinical Rehabilitation* 14 (Sept. 2000), pp. 408–416 (cit. on p. 7).
- [14] A. M. Owen, M. R. Coleman, M. Boly, M. H. Davis, S. Laureys, and J. D. Pickard. «Using Functional Magnetic Resonance Imaging to Detect Covert Awareness in the Vegetative State». In: *American Medical Association* 1098 (Aug. 2007) (cit. on pp. 10, 11).
- [15] A. M. Owen and M. R. Coleman. «Functional MRI in disorders of consciousness: advantages and limitations». In: *Current Opinion in Neurology* 20 (Jan. 2008), pp. 632–637 (cit. on p. 10).
- [16] D. Fernández-Espejo, T. Bekinschtein, M. M. Monti, J. D. Pickard, C. Junque, M. R. Coleman, and A. M. Owen. «Diffusion weighted imaging distinguishes the vegetative state from the minimally conscious state». In: *Science Direct* 54 (2011), pp. 103–112 (cit. on p. 12).
- [17] A. Comanducci et al. «Clinical and advanced neurophysiology in the prognostic and diagnostic evaluation of disorders of consciousness: review of an IFCN-endorsed expert group». In: *Science Direct* 131 (2020), pp. 2736–2765 (cit. on p. 13).
- [18] E. Lew, R. Chavarriaga, S. Silvoni, and J. del R. Millán. «Detection of self-paced reaching movement intention from EEG signals». In: *Frontiers in Neuroengineering* 5 (July 2012) (cit. on p. 16).
- [19] J. S. Kumar and P. Bhuvaneshwari. «Analysis of Electroencephalography (EEG) Signals and Its Categorization - A Study». In: *Procedia Engineering* 38 (2012), pp. 2525–2536 (cit. on pp. 17, 18).
- [20] M. Bracale, ed. *Elettromiografia*. Appunti del corso di Elettronica Biomedica. Napoli, Italy, 2002 (cit. on pp. 20–22).
- [21] L. Landini and A. Tognetti, eds. *Elettromiografia* (cit. on p. 22).
- [22] P. Haggard. «Conscious Intention and Motor Cognition». In: *Cognitive Science* 9 (June 2005), pp. 290–295 (cit. on pp. 23–25, 31, 32).
- [23] D. M. Wolpert and R. C. Miall. «Forward models for physiological motor control». In: *Neural Networks* 9 (1996), pp. 1265–1279 (cit. on p. 24).
- [24] H. Shibasaki and M. Hallett. «What is the Bereitschaftspotential?» In: *Clinical Neurophysiology* (Apr. 2006) (cit. on pp. 26–28).

- [25] C.Kranczioch, S. Mathews, P.J.A. Dean, and A. Sterr. «On the Equivalence of Executed and Imagined Movements: Evidence from Lateralized Motor and Nonmotor Potentials». In: *Human Brain Mapping* 30 (2009), pp. 3275–3286 (cit. on pp. 29, 30).
- [26] B. Libet, W.W. Elwood, and A.G. Curtis. «Readiness-potentials preceding unrestricted 'spontaneous' vs. pre-planned voluntary acts». In: *Neurophysiology of Consciousness* (1993), pp. 229–242 (cit. on pp. 30, 31).
- [27] G. Ouyang, W. Sommer, and C. Zhou. «Reconstructing ERP amplitude effects after compensating for trial-to-trial latency jitter: A solution based on a novel application of residue iteration decomposition». In: *International Journal of Psychophysiology* (Sept. 2016), pp. 9–20 (cit. on pp. 45, 47, 51, 78).
- [28] G. Ouyang, W. Sommer, and C. Zhou. «A toolbox for residue iteration decomposition (RIDE)— A method for the decomposition, reconstruction, and single trial analysis of event-related potentials». In: *Journal of Neuroscience Methods* (Oct. 2014), pp. 7–21 (cit. on pp. 45, 46, 54).
- [29] Marika Loglisci. «Event-related potentials' jitter compensation for Brain-Computer Interfaces applications». MA thesis. Torino: Politecnico di Torino, 2020 (cit. on p. 48).
- [30] SapienLabs. *Pitfalls of Filtering the EEG Signal*. 2018. URL: <https://sapienlabs.org/lab-talk/pitfalls-of-filtering-the-eeeg-signal> (cit. on p. 84).